101th USCAP Annual meeting, Mar 19-21, 2011, Vancouver, Canada

G. 知的財産権の出願・登録状況

1. 特許取得

なし

2. 実用新案登録

なし

3.その他

なし

厚生労働科学研究費補助金（第３次対がん総合戦略研究事業）
平成２１年度　分担研究報告書

ユーイング肉腫における新規膜抗原・分泌蛋白の探索に関する研究

分担研究者　野阪　哲哉　三重大学大学院医学系研究科　感染症制御医学分野　教授

研究要旨　　ユーイング肉腫（Ewing sarcoma）は若年者に好発する骨腫瘍である。化学療法の発達により予後は改善されつつあるが、依然不良であり、早期診断が望まれる。当研究ではシグナルシークエンストラップ法を用いて、ユーイング肉腫に特異的な新規膜抗原や分泌蛋白の探索スクリーニングを行い、*ADAMTS4*遺伝子を得た。同遺伝子はユーイング肉腫患者細胞で全例mRNA発現が見られたのに対し、骨肉腫患者細胞では一部の症例のみに見られ、診断への応用が示唆された。

Ａ．研究目的

ユーイング肉腫は1921年、ユーイングによって報告された高悪性度小円形細胞肉腫で、5-15歳で発症し、骨肉腫よりも若年者に好発する傾向がある。ユーイング肉腫の細胞起源は間葉系幹細胞、神経系細胞起源などが示唆されているが、詳細は不明である。骨の腫瘍であるにもかかわらず軟部への進展が速く、放射線や化学療法に対する反応はよいが、再発しやすく、骨や肺への転移のため、5年生存率は50%程度と悪性度が高い。ユーイング肉腫は、骨を覆っている軟部組織が厚いために早期発見が困難な場合も多い。このような若年性の難治性悪性腫瘍の克服は我が国における医学の重要課題のひとつであるが、そのためには、まず、早期に正確な診断をつけることが肝要である。

当研究においてユーイング肉腫特異的な分泌蛋白や膜蛋白、即ち、腫瘍マーカーを同定することは、上記目的を達成するための第一歩となる。将来的には分子標的療法への応用も視野に入れている。

Ｂ．研究方法

（レトロウイルスを用いたシグナルシークエンストラップ法によるユーイング肉腫特異的分泌蛋白、膜蛋白遺伝子の同定）

ユーイング肉腫由来のヒト細胞株（SJES-2, SJES-3, SJES-5, SJES-6, SJES-7, SJES-8）からmRNAを抽出し、レトロウイルスcDNA発現ライブラリーを作製し、当研究代表者らが開発したシグナルシークエンストラップ法（Kojima T & Kitamura T, Nat Biotechnol 1999）を用いて、膜蛋白、分泌蛋白を探索した。

（単離された遺伝子の発現解析）

得られたクローンのうち、組織特異性において興味深い発現パターンを示した遺伝子に関して、詳細に解析した。具体的には、細胞株、患者病変組織における当該遺伝子の発現を免疫組織染色で解析し、同時に患者細胞におけるRNA発現もRT-PCRにて解析した。また、ユーイング肉腫において頻繁に観察される*EWS-FLI1*融合遺伝子の発現が当該遺伝子の発現に及ぼす影響に関してもsiRNAを用いて解析した。さらに、ELISAにてユーイング肉腫患者血清や他疾患患者血清における当該遺伝子産物の濃度を解析した。

（倫理面への配慮）

当研究は、三重大学の研究倫理委員会の承認を得ている（No 1002）。臨床検体を用いる解析に関しては、その指針に従って該当者に説明を行い、同意書に署名をいただいた後、研究を行った。基本的には手術の際に摘出された検体や、検査のために採血された血清を、匿名性を保ったまま、患者様の同意のもとに一部使用させていただいたので、患者様の不利益や危険性はない。

Ｃ．研究結果

レトロウイルス発現系を用いたシグナルシークエンストラップ法にて80種類256クローンが単離された。これらのうち、明らかに組織特異的発現のない遺伝子や、他の組織の癌細胞で強く発現されているものは除外し、興味深い組織特異的mRNA発現パターンを示す遺伝子に焦点を絞ってさらに解析した。我々が最も注目したのは*ADAMTS4*遺伝子である。ADAMTS4は細胞外マトリックス蛋白質を分解するメタロプロテアーゼである。分泌蛋白であり、RT-PCR解析にて、正常マウス組織では脳において特異的に強く発現し、ヒト間葉系幹細胞での発現は検出されなかった。腫瘍細胞株では神経芽腫、横紋筋肉腫、ユーイング肉腫由来のものでmRNAの強い発現が検出された。

細胞株におけるADAMTS4の蛋白レベルでの発現を免疫組織化学染色法にて解析したところ、ユーイング肉腫細胞株（SJES-2, SJES-5）では細胞質で発現していたが、骨肉腫細胞株（MG63, SaOS2）では発現が検出されなかった。免疫沈降-Western法では前者細胞株において細胞抽出液、培養上清の両者からADAMTS4蛋白が検出された。臨床検体を用いた解析では、ユーイング肉腫患者の病変組織25検体中10検体でADAMTS4の発現が観察された。検出されなかった15検体は化学療法にて腫瘍が消失しているものであっ

た。患者細胞におけるRNA発現もRT-PCRにて解析したところ、骨肉腫2/13症例、ユーイング肉腫7/7症例、滑膜肉腫1/4症例、軟骨肉腫3/4症例で陽性であったが、横紋筋肉腫3症例、シュワン細胞腫、類腱腫、脂肪腫計6症例では検出されなかった。

また、ユーイング肉腫細胞株SJES-5において*EWS-FLI1*融合遺伝子の発現をsiRNAを用いてノックダウンしたところ、コントロールの遺伝子発現に比較して、*ADAMTS4*遺伝子の発現が有意に低下した。

最後に患者血清中におるADAMTS4蛋白の検出をELISAにて試みたが、ユーイング肉腫6症例、健常者4例、軟骨肉腫、滑膜肉腫各1症例全てにおいて検出感度以下であった。一方、骨肉腫2/3症例、骨線維性異形成1/1症例で陽性であった。

D．考察

上記の実験結果では、*ADAMTS4*の遺伝子発現がRT-PCRで見られないときは、ユーイング肉腫の可能性が低いと言えそうである。これは、骨肉腫との鑑別診断に役立つと思われる。

ADAMTS4は分泌蛋白であるが、血清中の蛋白レベルでの存在は、疾患の鑑別診断には役立たないことも判明した。腫瘍組織局所での働きが重要であるのかもしれない。ELISAの感度を改善すれば、予後との関連や病態の反映など、病態マーカー的に利用できるか、さらには、ADAMTS4がユーイング肉腫の病因に直接関与するのか、明らかにする必要がある。また、*EWS-FLI1*融合遺伝子産物が直接に*ADAMTS4*遺伝子の発現を調節しているのか、も今後の検討課題である。

E．結論

レトロウイルス発現クローニング法を用いたシグナルシークエンストラップ法にて6種のユーイング肉腫細胞株mRNAの混合物から、80種、256クローンの遺伝子を単離した。そのうちのひとつの遺伝子である*ADAMTS4*の、病変部でのmRNA発現の有無はユーイング肉腫と骨肉腫の鑑別診断に応用できる可能性が示唆された。

F．健康危険情報

該当せず。

G．研究発表

1．論文発表

1) Ikeya M, Fukushima K, Kawada M, Onishi S, Furuta Y, Yonemura S, Kitamura T, Nosaka T, Sasai Y. Cv2, functioning as a pro-BMP factor via twisted gastrulation, is required for early development of nephron precursors. Dev Biol 337: 405-414, 2010.

2) Jin G, Matsushita H, AsaiS, Tsukamoto H, Ono R, Nosaka T, Yahata T, Takahashi S, Miyachi H. FLT3-ITD induces ara-C resistance in myeloid leukemic cells through the repression of the ENT1 expression. Biochem Biophys Res Commun 390: 1001-1006, 2009.

3) Ono R, Kumagai H, Nakajima H, Hishiya A, Taki T, Horikawa K, Takatsu K, Satoh T, Hayashi Y, Kitamura T, Nosaka T. Mixed-lineage-leukemia (MLL) fusion protein collaborates with Ras to induce acute leukemia through aberrant Hox expression and Raf activation. Leukemia 23: 2197-2209, 2009.

4) Watanabe-Okochi N, Oki T, Komeno Y, Kato N, Yuji K, Ono R, Harada Y, Harada H, Hayashi Y, Nakajima H, Nosaka T, Kitaura J, Kitamura T. Possible involvement of RasGRP4 in leukemogenesis. Int J Hematol 89: 470-481, 2009.

5) Kawashima T, Bao YC, Minoshima Y, Nomura Y, Hatori T, Hori T, Fukagawa T, Fukada T, Takahashi N, Nosaka T, Inoue M, Sato T, Kukimoto-Niino M, Shirouzu, M, Yokoyama S, Kitamura T. A Rac GTPase activating protein MgcRacGAP is an NLS-containing nuclear chaperone in the activation of STAT transcription factors. Mol Cell Biol 29: 1796-1813, 2009.

2．学会発表

1) Ono R, Masuya M, Miyata E, Nakajima H, Kamisako T, Ito M, Suzuki K, Katayama N, Kitamura T, Nosaka T.(2009年10月1日 横浜) Malignant transformation by *MLL-ENL* fusion gene arises selectively from long-term hematopoietic stem cells. 第68回日本癌学会学術総会.

2) 小埜良一、桝屋正浩、宮田恵里、中島秀明、上迫努、伊藤守、鈴木圭、片山直之、北村俊雄、野阪哲哉.(2009年10月24日 京都) MLL-ENL融合遺伝子は造血幹細胞のみを標的として形質転換を生じる. 第71回日本血液学会学術集会.

3) 北川敬之、坂口直、仁儀明納、西村廣明、伊奈田宏康、駒田洋、鶴留雅人、野阪哲哉、保富康宏、河野光雄. (2009年10月26日 東京) パラインフルエンザ２型ウイルスベクターを用いたアトピー性疾患に対する遺伝子免疫療法. 第57回日本ウイルス学会学術集会.

4) 西尾真智子、大塚順平、鶴留雅人、野阪哲哉. (2009年10月27日 東京) ヒトパラインフルエンザ２型ウイルス (hPIV2) P蛋白上の核移行シグナル (NLS) と核外移行シグナル (NES)

の同定. 第57回日本ウイルス学会学術集会.

H. 知的財産権の出願・登録状況(予定を含む)

1. 特許取得
   なし
2. 実用新案登録
   なし
3. その他
   なし

研究成果の刊行に関する一覧表

雑誌

発表者氏名	論文タイトル名	発表誌名	巻号	ページ	出版年
Shibata-Minoshima, F	Identification of RHOXF2 (PEPP2) as a cancer-promoting gene by expression cloning.	Int J Oncology	40	93-98	2012
Kato, N	Two types of C/EBPa mutations play distinct roles in leukemogenesis: Lessons from clinical data and BMT models.	Blood	117	221-233	2011
K, Minobe	Expression of ADAMTS4 in Ewing's sarcoma.	Int J Oncology	37	569-581	2010
Kitano, H	Podoplanin expression in cancerous stroma induces lymphangiogenesis and predicts lymphatic spread and patient survival.	Arch Pathol Lab Med	134	1520-1527	2010

Identification of RHOXF2 (PEPP2) as a cancer-promoting gene by expression cloning

FUMI SHIBATA-MINOSHIMA[1,2*], TOSHIHIKO OKI[1,2*], NORIKO DOKI[1,2], FUMIO NAKAHARA[1,2], SHUN-ICHIRO KAGEYAMA[3], JIRO KITAURA[1,2], JUNYA FUKUOKA[3] and TOSHIO KITAMURA[1,2]

Divisions of [1]Cellular Therapy and [2]Stem Cell Signaling, the Institute of Medical Science, the University of Tokyo, 4-6-1 Shirokanedai, Minatoku, Tokyo 108-8639; [3]Department of Surgical Pathology, Toyama University, 2630 Sugitani, Toyama 930-0194, Japan

Received June 27, 2011; Accepted July 28, 2011

DOI: 10.3892/ijo.2011.1173

Abstract. Multiple mutations contribute to establish cancers. We have searched for potential oncogenes by screening cDNA libraries derived from gastric cancer cell lines, pancreatic cancer cell lines and glioma cell lines, using retrovirus-mediated expression cloning. Two types of interleukin-3 (IL-3)-dependent cell lines, Ba/F3 and HF6, were transduced with the cDNA libraries and several genes that render these cells factor-independent were identified including *PIM-1*, *PIM-2*, *PIM-3*, *GADD45B* and reproductive homeobox genes on the X chromosome gene F2 (*RHOXF2*). Although no mutation in these genes was found, these molecules were highly expressed in cancer cell lines and they may play important roles in cell transformation. Among them, we focused on a transcriptional repressor RHOXF2. Transduction of RHOXF2 rendered HF6 cells factor-independent, while knockdown of RHOXF2 inhibited growth of the HGC27 gastric cancer cell line which highly expresses RHOXF2. In addition, RHOXF2-transduced HF6 cells quickly induced leukemia when transplanted into sublethally irradiated mice. Moreover, RHOXF2 is highly expressed in some leukemia cell lines and a variety of human cancer samples including colon and lung cancers. Thus, these results indicate that RHOXF2 is involved in carcinogenesis.

Introduction

Cancer develops through a multistep process involving a variety of gene alterations and epigenetic changes (1,2). Genes that are commonly altered include Rb, $p16^{INK4a}$, VHL, Ras, p53 and APC (2,3). Fusion genes resulting from chromosomal translocations are established hallmarks of hematopoietic malignancies and include BCR-ABL, MLL-fusions and AML1-ETO (6). More recently, fusion genes have also been identified in solid tumors, for example EML4-ALK in lung cancer (4), EWS-FLI-1 in Ewing's sarcoma (5) and ETV6-NTRK3 in fibrosarcoma and breast cancer (6). Oncogenic mutations were originally identified using transfected NIH3T3 cells (7) in the focus-forming assay. A combination of the focus-forming assay with inoculation of NIH3T3 cells *in vivo* later increased the sensitivity to detect oncogenic potential (8). Recently, Soda *et al* identified a fusion gene EML4-ALK in non-small cell lung cancer by retrovirus-mediated expression cloning using transformation of the NIH3T3 cells as an assay (4). EML4-ALK is now a promising molecular therapeutic target; ALK inhibitors proved to be effective in the therapy for non-small cell lung cancer patients bearing this fusion gene (9). Detection of oncogenes has largely depended on the classical focus-forming assay with NIH3T3, which mainly detects activated mutations of Ras and gene alterations that activate the Ras pathway (7). To detect different classes of oncogenic mutations, different assays are likely to be required.

In this study, two hematopoietic cell lines, Ba/F3 (10) and HF6 (11), were used to search for potential oncogenes in several cancer types. Both cell lines are interleukin-3 (IL-3)-dependent early myeloid cells, but to become factor-independent, Ba/F3 requires JAK-STAT signaling and HF-6 requires Ras activation (11-13). Genes were tested for the ability to render these cell lines factor-independent. Using this strategy, several genes from cDNA libraries of gastric cancer cell lines, pancreatic cancer cell lines and glioma cell lines were identified including *PIM-1*, *PIM-2*, *PIM-3*, *GAD45B* and *RHOXF2*. Although mutations in these genes were not found, overexpression of *PIM-1*, *PIM-2*, *PIM-3*, *GAD45B* and *RHOXF2* rendered HF6 cells factor-independent, confirming the validity of the functional screening. Of the genes identified, we have focused on a homeobox protein, reproductive homeobox genes on the X chromosome F2 (RHOXF2), also known as PEPP2. Homeobox proteins, share a DNA-binding homeodomain motif of 60 amino acids, and are transcription factors that regulate development. The Rhox genes belong to a recently discovered homeobox family whose members are clustered on the X chromosome (14-16). Whereas the human RHOX family consists of three members, RHOXF1, RHOXF2 and RHOXF2B, the murine

Correspondence to: Dr Toshio Kitamura, Division of Cellular Therapy, the Institute of Medical Science, the University of Tokyo, 4-6-1 Shirokanedai, Minatoku, Tokyo 108-8639, Japan
E-mail: kitamura@ims.u-tokyo.ac.jp

*Contributed equally

Key words: c-DNA library screening, factor-independent growth, homeobox gene

Rhox family consists of >30 members (14-16). Rhox proteins are expressed in germ cells, embryonic cells and somatic cells of reproductive tissue, and play important roles in embryonic, postnatal and adult development, especially of the male and female reproductive systems. Recently, human and mouse Rhox protein expression in some cancer cells including breast and colon cancer was reported (16), and expression of a mouse Rhox family member, Rhox5, was found in 50-65% of cancer cells (17,18). Interestingly, Rhox protein expression is regulated by epigenetic mechanisms, and the treatment with DNA methyltransferase inhibitors, such as decitabine, induces Rhox expression (16). These findings indicate that Rhox proteins are involved in carcinogenesis. In the present study, it was found that knockdown of RHOXF2 attenuated the growth of a gastric cancer cell line HGC27 and overexpression of RHOXF2 in HF6 cells rapidly induced leukemia in transplanted mice. These results support a role for RHOXF2 in cell transformation.

Materials and methods

Cells. Human gastric cancer cell lines (HGC27, GCIY, KATOIII, MKN45, OCUM-1, AGS, MKN1, MKN7, MKN45, MKN74, NUGC3, SNU719, TMK-1), human pancreatic cancer cell lines (Bx-PC-3, AsPC-1, capan1) and human glioma cell lines (U87MG, T98G, U251) were maintained in Dulbecco's modified Eagle's medium (DMEM) supplemented with 10% fetal calf serum (FCS). Ecotropic and amphotropic retrovirus packaging cell lines, PLAT-E and PLAT-A respectively, were maintained in DMEM supplemented with 10% FCS, 1 μg/ml puromycin and 10 μg/ml blasticidin (19). A murine pro-B cell line Ba/F3 was maintained in RPMI-1640 with 10% FCS and 1 ng/ml mouse IL-3 (mIL-3), and a murine myelomonocytic cell line HF6 was maintained in RPMI-1640 with 20% FCS and 10 ng/ml mIL-3 (11).

Plasmids and primers. The coding region of RHOXF2 was amplified from HGC27 cDNA by PCR using Phusion polymerase (Finnzymes, Oy, Finland), then subcloned into pMXs-puro or pMXs-IG vectors (19,20) and the sequence was confirmed. Primers for RHOXF2 used in RT-PCR were as follows; (forward primer: cggaccagtgtagccagtat; reverse primer: tgacctcttcagtaagcgaca).

To generate shRNA vectors, first two oligonucleotides were designed using the siRNA Target Finder (Ambion Inc., Austin, USA) and were synthesized as follows; RHOXF2-1 (sense: ggca cagcagcaggagaaa, antisense: tttctcctgctgctgtgcc) and RHOXF2-2 (sense: gagccaaatggaggagaca, antisense: tgtctcctccatttggctc). These oligonucleotides were annealed and ligated to the pReps vector, which was kindly provided by T. Hara (21). Control shLuc vector targeting firefly luciferase was constructed in the same way.

Generation of anti-RHOXF2 antibody. Anti-RHOXF2 polyclonal antibody was generated from the serum of rabbits immunized with the purified GST-RHOXF2 fusion protein (Scrum Inc., Tokyo, Japan).

Retroviral gene transduction. Retroviral transduction was performed as described (19,20). Briefly, ecotropic and amphotropic retroviruses were generated by the packaging cell lines Plat-E and Plat-A, respectively, and then transiently transfected with a pMXs-based construct using FuGENE 6 reagent (Roche Applied Science, Basel, Switzerland). Two days after transfection, ecotropic and amphotropic retroviruses were collected and used to infect mouse HF6 cells or human HGC27 cells, respectively.

Screening of cDNA libraries. pMXs-based cDNA libraries were generated from gastric cancer cell lines, pancreatic cancer cell lines and glioma cell lines, as previously described (13). Each cDNA library was retrovirally introduced into two IL-3-dependent cell lines, Ba/F3 and HF6. Two days after transduction, the cells were seeded into 96-well plates in the absence of IL-3 in order to select factor-independent clones. To identify the cDNA that conferred Ba/F3 or HF6 cells with factor-independency, the integrated cDNAs were isolated from factor-independent clones by genomic PCR and were sequenced using primers specific to the retroviral vector sequence.

Soft agar colony formation. One thousand cells were suspended in 0.6% agar supplemented with complete culture medium. This suspension was layered over 1.2% agar-medium bottom layer in 35-mm dishes. After 14 days, colonies were counted.

Mouse bone marrow transplantation (BMT). One million HF6 cells transduced with empty (mock) or RHOXF2-containing retroviral vector were injected into the tail vein of sub-lethally irradiated (5.25 Gy) C57BL/6 (Ly-5.1) 8-week-old mice. Overall survival of the transplanted mice was analyzed using the Kaplan-Meier method. Animal studies were conducted in according to the guidelines of the Animal Care Committee at the Institute of Medical Science, University of Tokyo.

Generation of tissue microarray. Tissue microarrays (TMA) were generated from 1150 cases of 14 common cancer types as previously described (22). In addition, TMA composed of 280 non-neoplastic adjacent tissues from the same patients were made using identical methods. Each sample of TMA was cut in 4-μm section for immunohistochemical analysis. Tissue microarray methods in the present study were approved by the Ethics Committee of Toyama University (no. 19-12).

Immunohistochemical analysis of tissue microarrays. Immunohistochemical detection of RHOXF2, and statistical analyses of results were carried out as previously described (22). In short, after deparafinization and rehydration, sections were processed for heat-induced antigen retrieval at 125°C and incubated with diluted antibody (1:500) for 30 min at room temperature. Antibody staining was visualized using the Envision$^+$ system (Dako, Kyoto, Japan) and diaminobenzidine.

Nuclear staining was scored according to 4 grades (0, none; 1, mild; 2, moderate; 3, marked). Scores 0 and 1 were considered negative while scores 2 and 3 were considered positive. RHOXF2 staining of sections of an embedded pellet of HF6 cell line and colonic mucosa were used as positive and negative staining controls, respectively (data not shown).

Results

Expression cloning of potential oncogenes from cancer cell lines. cDNA was generated from gastric cancer cell lines,

Table I. Characteristics of c-DNA libraries.

	Gastric Cancer	Pancreatic cancer	Glioma
Cell lines	HGC-27, OCUM-1, MKN45, GCIY, KATOIII	BxPC-3, AsPC-1, capan1	U87MG, T98G, U251
Library size	$4.5x10^6$	$3x10^6$	$3x10^6$
Avarage length of cDNAs (kb)	1.2	1.4	1.3

The name of the cell lines used for making each library (cell lines), the numbers of independent cDNA clones of each library (library size), and the average length of the cDNAs included in each library (avarage length of cDNAs) are described.

Table II. Details of the isolated clones from screening.[a]

	Gastric	Pancreatic	Glioma
Total isolated clone	5	2	6
The clones with full ORF	*PIM-1,3, RNF67, RHOXF2*	*PIM-1, GADD45B*	*PIM-2,3, CSF3, GADD45B*
The clones with partial ORF	*TENC1, RAF1*		*FOXM1, ATXN1*
The candidate oncogenes	*PIM-1,3, RHOXF2*	*PIM-1, GADD45B*	*PIM-2,3, GADD45B*

[a]The clones isolated from 3 different c-DNA libraries are shown. The clones consist of two categories, the clones with full length of open reading frame (ORF) of cDNAs (the clones with full ORF) and the clones with partial sequence of ORF (the clones with partial ORF). The names of the genes which the clones of each category from 3 kinds of libraries contain, are shown in the table. Among the genes from the clones with full length ORF, some genes rendered HF6 factor-independent and the names of the genes are indicated in the table (the candidate oncogenes).

pancreatic cancer cell lines and glioma cell lines as described, and a cDNA library was constructed from the mixed cDNAs from each cancer in a retrovirus vector pMXs (20) (Table I). The resulting library was introduced into IL-3-dependent Ba/F3 cells and HF6 cells via retrovirus infection, and the infected cells were cultured in the absence of IL-3 to identify potential oncogenes that render the cells factor-independent. Several factor-independent clones were established from HF6 transfectants and *PIM-1*, *PIM-2*, *PIM-3*, *GADD45B* and *RHOXF2* were isolated from these clones by genomic PCR (Table II). These genes were introduced into HF6 cells and the ability of these genes to confer HF6 cells with autonomous growth was confirmed (data not shown). However, no mutation was found in these genes, indicating that overexpression of these genes alone could transform HF6 cells.

Expression of RHOXF1 and F2 in a variety of cell lines. The Rhox family consists of 30 members in mice and 3 members in humans, RHOXF1, F2 and F2B. Interestingly, expression of RHOXF1 and F2 was almost mutually exclusive in gastric cancer cells examined (Fig. 1A). HGC27 (undifferentiated carcinoma), NUGC3 (poorly differentiated adenocarcinoma) and TMK-1 (poorly differentiated adenocarcinoma) cell lines express RHOXF2 but not RHOXF1. On the other hand, GCIY (scirrhous), MKN1 (adeno-squamous), MKN7 (well differentiated adenocarcinoma), MKN74 (moderately differentiated adenocarcinoma) and SNU719 (well differentiated adenocarcinoma) cell lines express RHOXF1 but not RHOXF2. These results suggested complementary roles for RHOXF1 and F2.

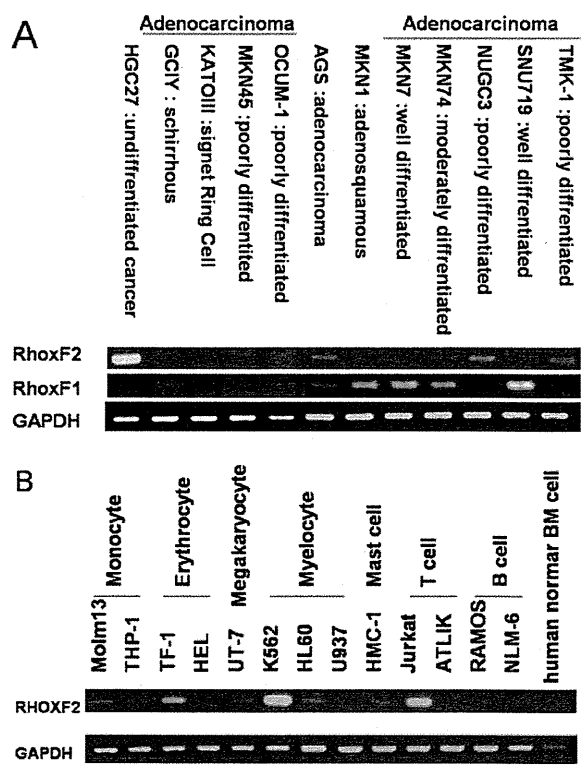

Figure 1. Expression of RHOXF2 in cancer cell lines. Expression of RHOXF2 was analyzed by RT-PCR. The expression in gastric cancer cell lines (A) and cell lines derived from hematological malignancies (B) are shown.

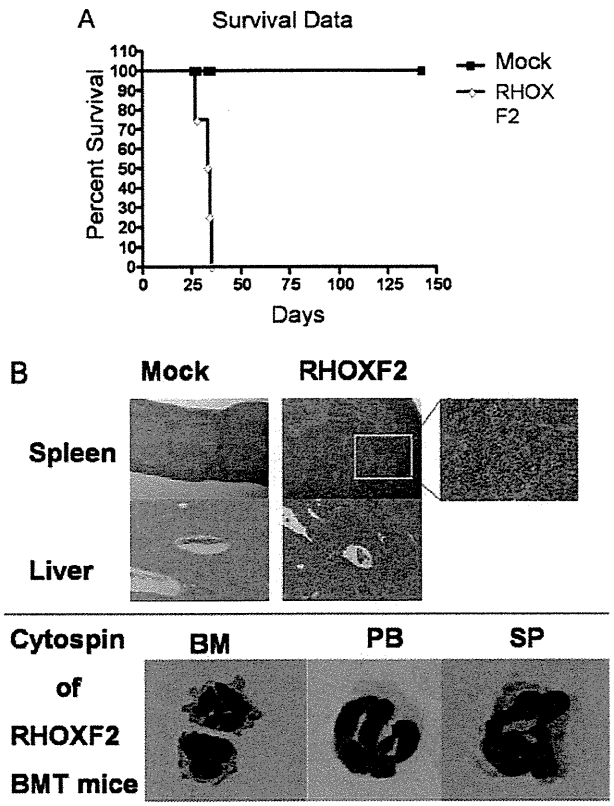

Figure 2. Leukemia-like disease was induced by HF6 transduced with RHOXF2 but not by parental HF6 cells. The effects of RHOXF2 overexpression were analyzed using a mouse BMT model. Kaplan-Meier survival curves for mice transplanted with HF6-mock cells (black squares) or HF6-RHOXF2-transfectants (white diamonds) are shown (A). Hematoxylin & eosin-stained histological samples and May-Giemsa-stained cytospins revealed that hepato-splenomegaly caused by a leukemia-like cell infiltration was observed in mice transplanted with HF6-RHOXF2-trasnfectants (B).

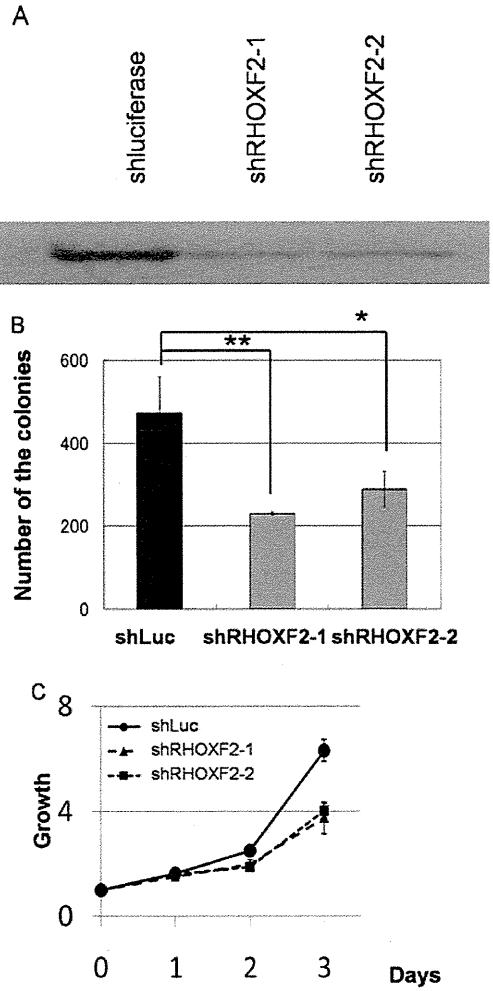

Figure 3. Knockdown of RHOXF2 attenuated the growth of a gastric cancer cell line, HGC27. Two shRNA vectors, shRHOXF2-1 and shRHOXF2-2, were designed to knockdown RHOXF2. Both shRNAs effectively inhibited the expression of RHOXF2 protein (A). shLuciferase vector was used as a control (shLuc). Colony formation in soft agar (B) and cell growth (C) of HGC27 transfectants were inhibited by shRHOXF2-1 (squares) and shRHOXF2-2 (triangles) but not by shLuc (circles). Statistical analysis was performed using the t-test; $^{*}P<0.05$, $^{**}P<0.01$. All experiments were conducted in triplicates. The result shown here is a representative of 3 independent experiments.

The undifferentiated to poorly differentiated gastric cancers tended to express RHOXF2, while the adenocarcinoma cell line AGS appeared to express both RHOXF1 and F2.

RHOXF2 was also highly expressed in the human immature leukemic cell lines including TF-1 and K562 (Fig. 1B). It was also expressed in the other human hematopoietic cell lines, MOLM13, UT-7, HL60, MHC-1 and Jurkat (Fig. 1B).

Effects of overexpression of RHOXF2 in HF6 cells. HF6 cells that were manipulated to express RHOXF2 proliferated autonomously *in vitro* in the absence of IL-3 (data not shown). Next the effects of RHOXF2 overexpression *in vivo* were examined using a mouse BMT model. While unmanipulated HF6 cells did not induce disease in 5 months after the transplantation into sub-lethally irradiated mice, HF6 cells expressing RHOXF2 rapidly induced leukemia-like disease (Fig. 2A). In these mice, the leukemic cells infiltrated to the liver and spleen, causing hepato-splenomegaly (Fig. 2B).

Effects of RHOXF2 knockdown in HGC27. Next, the effects of RHOXF2 knockdown were evaluated. To achieve this, shRNA specific for RHOXF2 was retrovirally introduced into HGC27 gastric cancer cells which express RHOXF2 at high levels (Fig. 3A). While the control shLuciferase did not inhibit the expression of RHOXF2, two RHOXF2 sh-RNA constructs efficiently suppressed the expression of RHOXF2 in HGC27 cells (Fig. 3A). Knockdown of RHOXF2 inhibited the colony forming ability of HGC27 cells in soft agar (Fig. 3B) and the growth rate in a liquid culture (Fig. 3C), implicating RHOXF2 in transformation and cell growth.

Expression of RHOXF2 in a multi-cancerous tissue microarray. Expression of RHOXF2 in a variety of cancers and non-neoplastic tissues was evaluated using two TMA blocks (Fig. 4). RHOXF2 was not highly expressed in any of the normal tissues tested except for thyroid. RHOXF2 was highly expressed in some of the cancers including lung squamous cell carcinoma, thyroid tumors, colon, breast, gastric, prostate, ovarian and uterine corpus cancers.

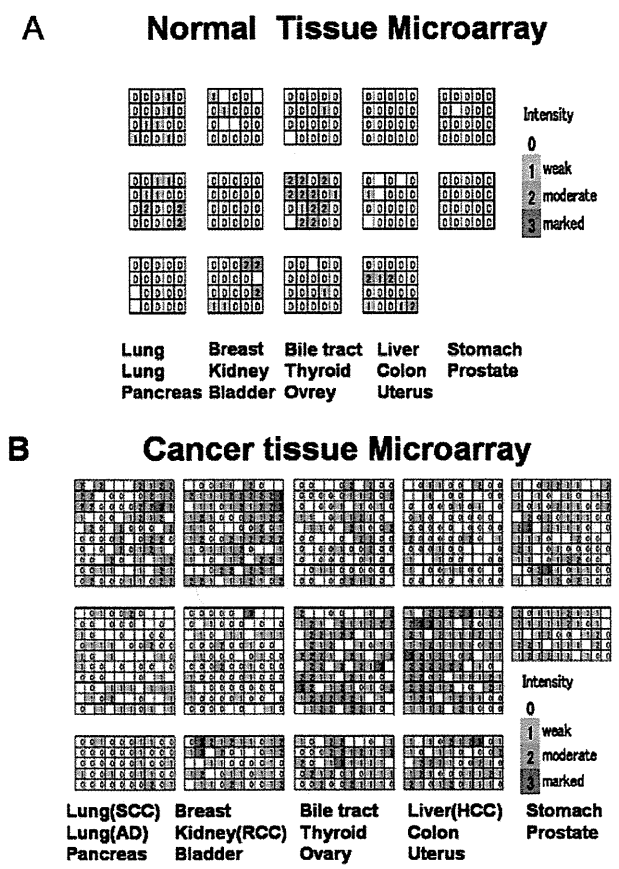

Figure 4. Tissue microarray analysis. Immunohistochemical analysis of RHOXF2 expression in multi-tissue array is shown. (A and B) The array contains 280 non-neoplastic tissue samples and 1150 tumor tissue samples from 14 major types of cancers. Each column represents each case and the number in the column indicates the score corresponding to the level of RHOXF2 expression.

Discussion

In the present work, a transcriptional repressor RHOXF2 has been identified as a potential oncogene by functional expression cloning. Knockdown of RHOXF2 inhibited the growth and colony forming ability of the gastric cancer cell line HGC27. On the other hand, overexpression of RHOXF2 conferred IL-3-dependent HF6 cells with autonomous growth and leukemogenicity *in vivo*. In addition, RHOXF2 expression was found in a variety of cancer tissues. Recently, several studies have reported that expression of RHOXF2 is regulated by some epigenetic mechanisms, especially in cancer tissues (16). These findings suggest that RHOXF2 plays a role in tumorigenesis and that it can be controlled epigenetically. To elucidate the molecular mechanisms, further studies using gene chips and bioinformatics are required to identify the responsive genes downstream of RHOXF2. HF6 is a mouse bone marrow-derived IL-3-dependent cell line immortalized by the fusion gene MLL-SEPT6, and activation of the Ras pathway in these cells can lead to transformation (11,13). Ras activation frequently plays an important role in carcinogenesis and it is possible that genes repressed or enhanced by RHOXF2 are involved in this pathway.

It is now recognized that as in solid tumors, multiple mutations are involved in the development of hematopoietic malignancies. These mutations are classified into two groups; class I mutations include activating mutations of tyrosine kinases and oncogenes, and inactivating mutations of tumor suppressor genes such as p53, NF1, while class II mutations include dominant-negative mutations of transcription factors and chromatin modification enzymes (23-25). We have previously demonstrated that a class II mutation MLL-SEPT6 could immortalize mouse bone marrow cells by blocking the differentiation of hematopoietic progenitors (11-13). However, these immortalized cells still require interleukin 3 (IL-3) for their growth. Interestingly, class I mutations such as those that activate Ras signal or constitutively active receptors tyrosine kinase mutants, like FLT3-ITD, were able to fully transform the IL-3-dependent HF6 cells immortalized by class II mutations (13).

The assay system using NIH3T3 cells has been the gold standard for screening of oncogenes, however this system mainly detects activators of the Ras pathway (7). For this reason, different cell types have been needed to be tested in the search for the oncogenic mutations. In the present study, HF6 cells and Ba/F3 cells were used. HF6 cells and Ba/F3 cells require activation of the Ras pathway and the JAK-STAT pathway, respectively, for the full transformation. In addition, we have established a cell line HF8 cells by introducing Hes1 to bone marrow progenitors. Neither Ras nor JAK/STAT activation could confer HF8 cells with autonomous growth (unpublished observation), indicating that these IL-3-dependent cell lines examined have distinct signaling profiles. The use of different cell lines could therefore, identify different classes of mutations. In the present study, *PIM-1*, *PIM-2*, *PIM-3*, *GADD45B* and *RHOXF2* were shown to render HF6 cells factor-independent, demonstrating the potential for using cells of hematopoietic origin to identify oncogenic mutations. It is possible that different types of mutations and translocations could be identified, using distinct types of IL-3-dependent cell lines.

In conclusion, the transcriptional repressor RHOXF2 is expressed in a variety of cancers, and plays a critical role in tumorigenesis. The use of IL-3-dependent cell lines for screening cDNA libraries has potential as a strategy in the search for oncogenes.

Acknowledgements

We thank Dr T. Hara for kindly providing the retrovirus shRNA vector (pReps), and Mr. Masunori Kajikawa, ACTGen Inc., (Komagane, Japan) for providing cancer cell lines. This work was supported by grants from the Ministry of Health, Labor and Welfare.

References

1. Hanahan D and Weinberg RA: The hallmarks of cancers. Cell 100: 57-70, 2000.
2. Esteller M: Epigenetics in cancer. N Eng J Med 358: 1148-1159, 2008.
3. Jones PA and Baylin SB: The fundamental roles of epigenetic events in cancer. Nat Rev Genet 3: 415-428, 2002.
4. Soda M, Choi YL, Enomoto M, *et al*: Identification of the transforming EML4-ALK fusion gene in non-small-cell lung cancer. Nature 448: 561-566, 2007.

5. Delattre O, Zucman J, Plougastel B, *et al*: Gene fusion with an *ETS* DNA-binding domain caused by chromosome translocation in human tumours. Nature 359: 162-169, 1992.
6. Mitelman F, Johansson B and Mertens F: Fusion genes and rearranged genes as a linear function of chromosome aberration in cancer. Nat Genet 36: 331-334, 2004.
7. Clark GL, Cox AD, Graham SM and Der CJ: Biological assays for Ras transformation. Method Enzymol 255: 395-412, 1995.
8. Takahashi K, Mitsui K and Yamanaka S: Role of ERas in promoting tumour-like properties in mouse embryonic stem cells. Nature 423: 541-545, 2003.
9. Gerber DE and Minna JD: ALK inhibition for non-small cell lung cancer: from discovery to therapy in record time. Cancer Cell 18: 548-551, 2010.
10. Palacios R and Steinmetz M: IL3-dependent mouse clones that express B-220 surface antigen, contain ig genes in germ-line configuration, and generate B lymphocytes in vivo. Cell 41: 727-734, 1985.
11. Ono R, Nakajima H, Ozaki K, *et al*: Dimerization of MLL fusion proteins and FLT3 activation synergize to induce multiple-lineage leukemogenesis. J Clin Invest 115: 919-929, 2005.
12. Onishi M, Nosaka T, Misawa K, *et al*: Identification and characterization of a constitutively active STAT5 mutant that promotes cell proliferation. Mol Cell Biol 18: 3871-3879, 1998.
13. Watanabe-Okochi N, Oki T, Komeno Y, *et al*: Possible involvement of RasGRP4 in leukemogenesis. Int J Hematol 89: 470-481, 2009.
14. Maclean JA II, Chen MA, Wayne CM, *et al*: Rhox: a new homobox gene cluster. Cell 120: 369-382, 2005.
15. MacLean JA II and Wilkinson MF: The Rhox genes. Reproduction 140: 195-213, 2010.
16. Li Q, Bartlett DL, Gorry MC, O'Malley ME and Guo ZS: Three epigenetic drugs up-regulate homeobox gene Rhox5 in cancer cells through overlapping and distinct-molecular mechanisms. Mol Pharmacol 76: 1072-1081, 2009.
17. Wilkinson MF, Kleeman J, Richards J and MacLeod CL: A novel oncofetal gene is expressed in a stage-specific manner in murine embryonic development. Dev Biol 141: 451-455, 1990.
18. Ono T, Sato S, Kimura N, *et al*: Serological analysis of BALB/C methylcholanthrene sarcoma Meth A by SEREX: identification of a cancer/testis antigen. Int J Cancer 88: 845-851, 2000.
19. Morita S, Kojima T and Kitamura T: Plat-E: an efficient and stable system for transient packaging of retroviruses. Gene Ther 7: 1063-1066, 2000.
20. Kitamura T, Koshino Y, Shibata F, *et al*: Retrovirus-mediated gene transfer and expression cloning: powerful tools in functional genomics. Exp Hematol 31: 1007-1014, 2003.
21. Fujino RS, Tanaka K, Morimatsu M, Tamura K, Kogo H and Hara T: Spermatogonial cell-mediated activation of an IκBζ-independent nuclear factor-κB pathway in sertoli cells induces transcription of the lipocalin-2 gene. Mol Endcrinol 20: 904-905, 2006.
22. Kitano H, Kageyama S, Hewitt SM, *et al*: Podoplanin expression in cancerous stroma induces lymphangiogenesis and predicts lymphatic spread and patient survival. Arch Pathol Lab Med 134: 1520-1527, 2010.
23. Gilliland DG: Molecular genetics of human leukemias: new insights into therapy. Semin Hematoi 39: 6-11, 2002.
24. Dash A and Gilliland DG: Molecular genetics of acute myeloid leukaemia. Best Pract Res Clin Haematol 14: 49-64, 2001.
25. Renneville A, Roumier C, Biggio V, *et al*: Cooperating gene mutations in acute myeloid leukemia: a review of the literature. Leukemia 22: 915-993, 2003.

Two types of C/EBPα mutations play distinct but collaborative roles in leukemogenesis: lessons from clinical data and BMT models

Naoko Kato,[1,2] Jiro Kitaura,[1] Noriko Doki,[1] Yukiko Komeno,[1] Naoko Watanabe-Okochi,[3] Katsuhiro Togami,[1] Fumio Nakahara,[1,2] Toshihiko Oki,[1,2] Yutaka Enomoto,[1] Yumi Fukuchi,[4] Hideaki Nakajima,[4] Yuka Harada,[5] Hironori Harada,[6] and Toshio Kitamura[1,2]

Divisions of [1]Cellular Therapy and [2]Stem Cell Signaling, Institute of Medical Science, University of Tokyo, Tokyo, Japan; [3]Department of Hematology and Oncology, Graduate School of Medicine, University of Tokyo, Tokyo, Japan; [4]Division of Hematology, Department of Internal Medicine, Keio University School of Medicine, Tokyo, Japan; [5]International Radiation Information Center, Research Institute for Radiation Biology and Medicine, Hiroshima University, Hiroshima, Japan; and [6]Department of Hematology and Oncology, Research Institute for Radiation Biology and Medicine, Hiroshima University, Hiroshima, Japan

Two types of mutations of a transcription factor CCAAT-enhancer binding protein α (C/EBPα) are found in leukemic cells of 5%-14% of acute myeloid leukemia (AML) patients: N-terminal mutations expressing dominant negative p30 and C-terminal mutations in the basic leucine zipper domain. Our results showed that a mutation of C/EBPα in one allele was observed in AML after myelodysplastic syndrome, while the 2 alleles are mutated in de novo AML. Unlike an N-terminal frame-shift mutant (C/EBPα-N^m)–transduced cells, a C-terminal mutant (C/EBPα-C^m)–transduced cells alone induced AML with leukopenia in mice 4-12 months after bone marrow transplantation. Coexpression of both mutants induced AML with marked leukocytosis with shorter latencies. Interestingly, C/EBPα-C^m collaborated with an Flt3-activating mutant Flt3-ITD in inducing AML. Moreover, C/EBPα-C^m strongly blocked myeloid differentiation of 32Dcl3 cells, suggesting its class II mutation-like role in leukemogenesis. Although C/EBPα-C^m failed to inhibit transcriptional activity of wild-type C/EBPα, it suppressed the synergistic effect between C/EBPα and PU.1. On the other hand, C/EBPα-N^m inhibited C/EBPα activation in the absence of PU.1, despite low expression levels of p30 protein generated by C/EBPα-N^m. Thus, 2 types of C/EBPα mutations are implicated in leukemogenesis, involving different and cooperating molecular mechanisms. (*Blood.* 2011; 117(1):221-233)

Introduction

The CCATT/enhancer binding protein α (C/EBPα) transcription factor is a critical regulator of proliferation and differentiation in myeloid cells.[1,2] C/EBPα consists of an N-terminal transcriptional activation domain and a C-terminal basic leucine zipper (bZIP) domain.[3-5] Two isoforms of C/EBPα proteins are generated from different translation start sites: a full-length 42-kDa protein (p42) and a truncated 30-kDa protein (p30) that lacks an N-terminal transcriptional activation domain. C/EBPα-p30 isoform inhibits C/EBPα-p42–mediated transcription.[6-8] Importantly, C/EBPα promotes differentiation both by up-regulation of lineage-specific gene products[9-11] and by proliferation arrest.[12] Recent studies have indicated that C/EBPα-induced growth arrest is regulated by its interaction with other molecules involved in growth control: E2F,[13-15] Max,[16] and SWI/SNF chromatin remodeling complexes.[17] For example, repression of E2F activity by E2F-C/EBPα interaction results in the down-regulation of c-Myc, leading to granulocytic differentiation.[18,19]

According to several studies, *CEBPA* mutations are found in 5%-14% of acute myeloid leukemia (AML) patients belonging to the French-American-British subtypes M1, M2, or in some cases M4.[8,20-22] The mutations of the *CEBPA* gene can be largely categorized into 2 types: one is an N-terminal frame-shift mutation disrupting p42 and producing p30 as a major product, and the other is a C-terminal in-frame mutation disrupting the bZIP region. Interestingly, most AML patients with *CEBPA* mutations have both mutations simultaneously,[23-25] and such patients displayed a favorable outcome.[22,26] On the other hand, AML patients with single *CEBPA* mutations did not express a distinctive signature, presumably due to a variety of associating gene alterations, including Flt3 activating mutations. Related to this, involvement of single *CEBPA* mutations with myelodysplastic syndrome (MDS) remains to be clarified.[27,28]

Analysis of mice with genetic alterations in the *CEBPA* locus has contributed to delineation of molecular mechanisms by which *CEBPA* mutations induce leukemia. Conditional deficiency of C/EBPα led to a differentiation block at the transition between common myeloid progenitors and granulocyte/monocyte progenitors but not to development of leukemia.[1] However, $Cebpa^{L/L}$ mice, expressing only p30 as C/EBPα protein, developed myeloid leukemia with complete penetration.[29] On the other hand, $Cebpa^{BRM2/BRM2}$ mice, carrying a point mutation in the bZIP domain that dampened E2F interaction, showed only preleukemic features.[14] Interestingly, the same group has recently reported combinational effects of the C-terminal and the N-terminal mutations on leukemogenesis by using $Cebpa^{L/L}$ mice, $Cebpa^{K/K}$ mice carrying the K313 duplication in the C-terminal domain, and $Cebpa^{K/L}$ mice.[29,30] They proposed that efficient leukemogenesis is caused by the combination of both premalignant HSC expansion induced by

Submitted February 17, 2010; accepted September 22, 2010. Prepublished online as *Blood* First Edition paper, September 30, 2010; DOI 10.1182/blood-2010-02-270181.

The online version of this article contains a data supplement.

The publication costs of this article were defrayed in part by page charge payment. Therefore, and solely to indicate this fact, this article is hereby marked "advertisement" in accordance with 18 USC section 1734.

C-terminal *CEBPA* mutation and residual myeloid lineage commitment maintained by the N-terminal *CEBPA* mutation.[30]

Causative gene alterations in hematologic malignancies have been extensively studied, and it is now recognized that multiple mutations contribute to development of leukemia. These gene alterations are categorized into 2 groups, class I and class II mutations.[31,32] Class I mutations include activating mutations of *FLT3*, *C-KIT*, *JAK2*, *SHP2*, and *RAS*, or inactivating mutations of *TP53* and *NF-1*, and induce proliferation or block apoptosis of hemopoietic cells. On the other hand, class II mutations disrupt normal functions of transcription factors and chromosome-modifying enzymes including *MLL*, *RUNX1*, *RARA*, and *PU.1* and hamper differentiation of hemopoietic cells. Combinations of class I and class II mutations are frequently observed in patients' leukemic cells.[33,34] In addition, we and others presented evidence that class I and class II mutations collaborate in the development of leukemia in mouse models.[35,36] Among a variety of gene alterations found in leukemia, *CEBPA* mutations are unique because different *CEBPA* mutations are frequently found on different alleles in leukemic cells of de novo AML.[22-26]

In the present study, we searched for mutations of the *CEBPA* gene in patients with myeloid malignancies, and found N- and C-terminal double mutations in patients with de novo AML. In patients with MDS/AML or therapy-related AML or MDS, only N- or C-terminal single mutation was identified. We chose a C-terminal mutation 304_323dup (hereafter called C/EBPα-C^m) and an N-terminal mutation (T60fsX159) (hereafter C/EBPα-N^m) for further analysis that had been isolated as double *CEBPA* mutations in a de novo AML patient. To evaluate the effects of these mutations on leukemogenesis, we used a mouse bone marrow transplantation (BMT) model. Interestingly, unlike the phenotype in $Cebpa^{K/K}$, $Cebpa^{K/+}$, $Cebpa^{BRM2/BRM2}$, or $Cebpa^{BRM2/+}$ mice,[14,29,30] C/EBPα-C^m alone induced AML with leukopenia in transplanted mice after BMT. We also confirmed the efficient induction of AML by coexpression of C/EBPα-C^m and C/EBPα-N^m. We will discuss the possible molecular mechanisms by which C/EBPα-N^m worked in concert with C/EBPα-C^m in accelerating leukemogenesis.

Methods

Patients and samples

We chose patients with hematologic diseases (224 MDS/AML patients, 71 therapy-related AML or MDS patients, and 89 de novo AML patients, who had been diagnosed at Hiroshima University Hospital between 1985 and 2007, are not a consecutive series of patients). All studies were approved by the Institutional Review Board at Hiroshima University and the ethics committee of the University of Tokyo (approval no. 20-10-0620). Patients' informed consents were obtained in accordance with the Declaration of Helsinki. *CEBPA* mutation screening by polymerase chain reaction (PCR)–single strand conformation polymorphism analysis and identification of *CEBPA*, *AML1*, *N-RAS*, *FLT3*, *PTPN11*, *C-KIT*, and *TP53* mutations was performed as described previously.[37]

Retroviral vectors

We used 2 C/EBPα mutants, N^m or C^m, as well as C/EBPα wild-type (WT) and C/EBPα N-terminal truncated p30 (p30). C/EBPα-WT, p30, N^m, or C^m, which was tagged with a FLAG or Myc epitope at the C terminus, was inserted upstream of the internal ribosome entry site-enhanced green fluorescent protein (IRES-EGFP) cassette of pMYs-IG to generate pMYs-FLAG or Myc-tagged CEBPα-WT, p30, N^m, or C^m-IG, respectively. Similarly, these fragments were subcloned into pMXs-IRES-puro (pMXs-IP), pMXs-IRES-blasticidin (pMXs-IB), or pMYs-IRES-dsRED (pMYs-IR). Flt3-ITD cDNA, which was derived from patient's leukemic cells harboring a 20-amino acid tandem duplication called M3[38,39] was subcloned into pMYs-IG to generate pMYs-Flt3-ITD-IG. Human granulocyte colony-stimulating factor receptor (G-CSF-R) cDNA, a kind gift from Dr Shigekazu Nagata (Kyoto University, Kyoto, Japan), was subconed into pMXs-IB to generate pMXs-G-CSF-R-IB.

Retroviral infection was done as described previously.[40] Briefly, retroviruses were generated by transient transfection of Plat-E packaging cells with FuGENE 6 (Roche Diagnostics).[41,42] Growth of transduced 32Dcl3 cells, which were subject to the drug selection with 1 μg/mL puromycin or 10 μg/mL blasticidin, was estimated by quantitating luminescence as described previously.[43]

Flow cytometric analysis

Briefly, cells were stained with phycoerythrin-conjugated antibodies (Abs) or biotinylated Abs and phycoerythrin/Cy5-streptavidin (eBioscience). Flow cytometric analysis of the stained cells was performed with FACSCalibur flow (BD Biosciences) equipped with FlowJo Version 7.2.4 software (TreeStar).

Real-time reverse-transcription PCR

Real-time reverse-transcription (RT) PCR was performed as described previously.[40] Reaction was subject to one cycle of 95°C for 30 seconds, 45 cycles of PCR at 95°C for 5 seconds, 55°C for 10 seconds, and 72°C for 10 seconds. The following primer pairs were used: 5′-AAGGCCCAGTGTGTCTCTGT-3′ (forward), and 5′-TACCAGCCCCAACTCAAAAC-3′ (reverse) for G-CSF-R, 5′-AGAGGGAAATCGTGCGTGAC-3′ (forward), and 5′-CAATAGTGATGACCTGGCCGT-3′ (reverse) for β-actin, 5′-GCCCCTAGTGCTGCATGAG-3′ (forward) and 5′-CCACAGACACCACATCAATTTCTT-3′ (reverse) for c-Myc.

Western blot analysis

Equal numbers of cells were lysed and Western blotting was performed as described previously.[35,40] Anti-Flag (M2) Ab (Sigma-Aldrich), anti-c-Myc (9E10) Ab (Roche Diagnostics), anti-C/EBPα (14AA) or (N-19) Ab (Santa Cruz Biotechnology), ERK1/2, signal transducer and activator of transcription (STAT)3, STAT5, AKT1, or Flt3 Abs, and phospho-STAT3 Ab (Santa Cruz Biotechnology), anti-phospho mitogen-activated protein kinase and phospho-AKT Abs (Cell Signaling Technology), and phospho-STAT5 Ab (BD Biosciences) were used.

Luciferase assay

The 293T cells were transiently transfected with the luciferase reporter plasmid p(C/EBP)2TK (kindly provided by Atsushi Iwama, Chiba University, Japan), pMXs-C/EBPα-WT or mutants-IP, and pEF-BOS/PU.1 for C/EBPα transcriptional activity, or E2Fx6-TATA-LUC, pCMV-E2F1, and pCMV-DP1 (kindly provided by Claus Nerlov, EMBL Mouse Biology Unit, Italy) for E2F transcriptional activity.[15] Luciferase assays were performed by Dual luciferase assay systems (Promega).

Immunostaining

Immunostaining of 293T cells transiently transfected with retrovirus constructs was performed as described previously.[35] After fixation with 1.5% paraformaldehyde, cells were immunostained with rabbit anti-Flag Ab or fluorescein isothiocyanate–conjugated mouse anti–c-Myc Ab (Sigma-Aldrich). The cells were then stained with Alexa Fluor 546–conjugated goat anti–rabbit immunoglobulin G secondary Ab (Molecular Probes). Nuclei were counterstained with Hoechst (H33342). Fluorescent images were analyzed on a confocal microscope (FLUOVIEW FV300 scanning laser biological microscope JX70 system; Olympus) equipped with SenSys/0L cold charge-coupled device (CCD) camera (Olympus). The objective lens (an LCPlanFI 60×/1.40 NA oil) was used.

Gel shift assay

Nuclear extracts from transfected 293T cells were incubated with 2 μg of polydeoxyinosinic-deoxycytidylic acid and then with double-stranded

Table 1. Clinical features and genetic findings of the patients with *CEBPA* mutations

Patient no.	Age, y/sex	Diagnosis	N terminal	C terminal		Karyotype	Other gene mutation*	Survival (years)
			p30 type	bZIP inframe	Frameshift			
MDS/AML								
142	79/F	AML following MDS	I62fsX160	-	-	46,XY[20/20]	-	1.0
829	70/M	AML following MDS	P51fsX160	-	-	45,XY,der(17;18)(q10;q10)[2/20]/46,XY[18/20]	-	0.4
769	69/M	AML following MDS	-	R297P	-	46,XY[20/20]	*AML1, PTPN11*	1.6
896	77/M	AML following MDS	-	K313del	-	46,XY[20/20]	-	0.6
22	71/M	AML following MDS	-	-	G176fsX317	47,XY,+1,der(1;15)(q10;q10)[20/20]	-	0.8
679	89/M	MDS(RAEB)	-	-	P235fsX318	46,XY[20/20]	-	1.9
806	77/M	AML following MDS	G38fsX107	-	R291fsX313	46,XY[20/20]	-	1.9
Therapy-related AML or MDS								
59	80/F	AML(M4)	L19fsX159	-	-	47,XX,+8,t(9;11)(p22;q23)[20/20]	*AML1*	1.7
158	72/F	AML following MDS	F106fsX154	-	-	46,XX[20/20]	-	1.0
811	76/M	MDS(RAEB)	E59X†	-	-	46,XY[20/20]	-	1.7
1068	66/M	MDS(RAEB)	-	Q305P	-	46,XY[20/20]	-	> 1.5
346	59/M	AML following MDS	-	-	S190fsX320	43,XX,del(5)(q31),-7,-15,-18,-21,+mar [20/20]	*N-RAS*	0.8
577	56/F	AML following MDS	-	-	C213X	46,XX[20/20]	-	2.4
629	89/F	AML following MDS	-	-	L350fsX360	46,XX[20/20]	-	1.2
920	69/F	AML(M5)	-	-	S348fsX422	46,XX,t(11;17)(p15;q21)[20/20]	-	0.2
De novo AML(M2)								
40	68/F	AML(M2)	A111fsX166	S299_L304dup	-	46,XX[20/20]	-	> 10.5
292	75/F	AML(M2)	F33fsX107	R297P	-	46,XX[20/20]	-	> 8.4
662	58/F	AML(M2)	S65fsX167	K313dup	-	46,XX[20/20]	-	> 5.0
888	70/F	AML(M2)	A111fsX166	N321D	-	47,XX,+8[20/20]	-	> 3.8
941	31/F	AML(M2Eo)	T60fsX159	304_323dup	-	46,XX,del(7)(q32)[20/20]	-	> 3.5

RAEB indicates refractory anemia with excess blasts.
*Indicates that no mutation was detected in *AML1*, *N-RAS*, *FLT3*, *PTPN11*, *C-KIT*, and *TP53* genes.
†Homozygous mutation.

CSF3R promoter oligonucleotide labeled with γ^{32}P-adenosine triphosphate. Cold competition and a super-shift reaction were carried out by adding a 40-fold excess of cold CSF3R oligo or 1.5 μg of anti-C/EBP (14AA)X Ab (Santa Cruz Biotechnology), respectively. The resulting complexes were resolved on 4.5% polyacrylamide gel.[44]

Colony assay

Infected mouse bone marrow (BM) mononuclear cells (1×10^4) were plated in methylcellulose medium (StemCell Technologies) supplemented with 50 ng/mL each of interleukin (IL)–3, IL-6, stem cell factor, and granulocyte/macrophage-colony-stimulating factor (GM-CSF; R&D Systems) in the presence of 1 μg/mL puromycin. Colonies were counted after 1-week culture, and single-cell suspensions (10^4 cells) of drug-resistant colonies were subsequently replated.

Mouse BMT

Mouse BMT was performed as described previously.[40] Briefly, BM mononuclear cells were isolated from the femurs and tibias of C57BL/6 (Ly-5.1) donor mice 4 days after intraperitoneal administration of 150 mg/kg 5-fluorouracil. The cells were stimulated with 50 ng/mL of mouse stem cell factor, mouse FLT3 ligand, mouse IL-6, and human thrombopoietin (all cytokines were from R&D Systems). The prestimulated cells were infected for 60 hours with the retroviruses harboring pMYs-C/EBPα-C^m-IG, pMYs-C/EBPα-N^m-IG, pMYs-Myc-tagged C/EBPα-C^m-IG, pMYs-Flag-tagged C/EBPα-N^m-IR, pMYs-Flt3-ITD-IG, pMYs-IG, or pMYs-IR, using 6-well dishes coated with RetroNectin (Takara Bio). Then, 3-5 × 10^5 of the infected BM cells (that had not been sorted after either single or double infection) were injected into sublethally γ-irradiated C57BL/6 (Ly-5.2) recipient mice. Overall survival of transplanted mice were estimated using the Kaplan-Meier method. All animal studies were approved by the Animal Care Committee of the Institute of Medical Science, The University of Tokyo.

Statistical analysis

Statistical significance was calculated using the Student *t* test for independent variables. *P* values < .05 were considered statistically significant.

Results

CEBPA mutations in patients with myeloid malignancies

After we performed single-strand conformation polymorphism analysis to screen for *CEBPA* mutations in patients with hematologic disorders, *CEBPA* mutations were identified in 7 of 224 MDS/AML patients, 8 of 71 therapy-related AML or MDS patients, and 5 of 89 de novo AML patients (Table 1). Although the number of the de novo AML patients with *CEBPA* mutations were small, they all carried both an N-terminal mutation and a C-terminal bZIP in-frame mutation on the different alleles as reported previously.[20-26] On the other hand, most MDS/AML or therapy-related AML or MDS patients had single *CEBPA* mutations. As exceptions, we found both an N-terminal mutation and a

C-terminal frame-shift mutation in 1 case of AML after MDS (patient [Pt] #806) and homozygous N-terminal frame-shift mutations in one case of therapy-related MDS/RAEB (Pt #811). Examination of other genes (*RUNX1, N-RAS, FLT3, PTPN11, C-KIT,* and *TP53* gene) in these patients demonstrated that one case of MDS/AML (Pt #769) had both *RUNX1* and *PTPN11* mutations and that patients with therapy-related AML or MDS (Pt #59 or #346) had a mutation of *RUNX1* or of *N-RAS*, respectively. Consistent with recent reports,[22,26] our clinical data showed that overall survival was better in de novo AML patients with double *CEBPA* mutations compared with others with single *CEBPA* mutations (Table 1). These results suggested that double *CEBPA* mutations were able to induce AML, whereas single *CEBPA* mutation would lead to more aggressive AML, in concert with other gene alterations that have not been fully characterized.

The C-terminal but not N-terminal mutations of C/EBPα inhibited G-CSF–induced differentiation of 32Dcl3 cells into mature neutrophils

For further analysis, we chose an N-terminal mutant producing p30 designated as C/EBPα-N^m and a C-terminal b-ZIP in-frame mutant designated as C/EBPα-C^m (Figure 1A). C/EBPα-WT, C/EBPα-N^m, C/EBPα-C^m, C/EBPα-p30, or mock (pMXs-IP) was expressed in Plat-E cells. Expression of p42 protein or p30 protein generated by Myc-tagged C/EBPα-WT and mutants was verified by using anti-Myc Ab as bands corresponding to expected molecular weights (Figure 1B). In addition, we confirmed that N-terminal polypeptide produced by C/EBPα-N^m was detected by anti-C/EBPα Ab recognizing the N-terminal portion of C/EBPα (supplemental Figure 1, available on the *Blood* Web site; see the Supplemental Materials link at the top of the online article). Notably, the expression levels of p30 generated by C/EBPα-N^m were lower than those generated by C/EBPα-p30 (Figure 1B), indicating that deletion of the N-terminal part including the first start codon might increase the expression levels of p30 protein. We then infected 32Dcl3 cells with retroviruses harboring C/EBPα-WT or mutants, and the infected cells were subjected to drug selection. The 32Dcl3 cells expressing detectable levels of C/EBPα-WT were not obtained, presumably due to its strong inhibitory effect on proliferation. Western blot analysis showed that 32Dcl3 cells transduced with C/EBPα-C^m expressed the full length of C/EBPα-C^m at high levels (Figure 1B). C/EBPα-N^m or C/EBPα p30 transduced into 32Dcl3 cells was detected as a band (30 kDa), but the expression level of the former was much lower than that of the latter (Figure 1B). Growth speed was comparable among these transfectants in the presence of IL-3 (Figure 1C). However, the potential of these transfectants to differentiate in response to G-CSF varied; G-CSF treatment induced terminal differentiation of 32Dcl3 cells transduced with mock, as indicated by the appearance of polymorphonucleated neutrophils and up-regulation of CD11b on the surface (Figure 1D-E). G-CSF–induced granulocytic differentiation of 32Dcl3 cells was profoundly inhibited by C/EBPα-C^m, while it was only weakly inhibited by C/EBPα-N^m (Figure 1D-E). The differentiation was also attenuated by C/EBPα-p30, as reported previously.[45] We reasoned that the difference of 32Dcl3 cells expressing C/EBPα-N^m or C/EBPα-p30 in the granulocytic differentiation levels was due to the dissimilar expression levels of a short form of C/EBPα (30 kDa). As for the expression levels of G-CSF-R transcripts, a target of C/EBPα, they were extremely or moderately decreased in 32Dcl3 cells expressing C/EBPα-C^m or C/EBPα-p30, respectively, compared with other transfectants (Figure 1F), implicating G-CSF-R in induction of granulocytic differentiation. However, when human G-CSF-R was transduced into C/EBPα-C^m-expressing 32Dcl3 cells, G-CSF–induced granulocytic differentiation was not completely recovered (supplemental Figure 2). These results indicated that the differentiation block in 32Dcl3 cells expressing C/EBPα-C^m was presumably due to the suppression of C/EBPα activation, but not simply due to the decreased expression of G-CSF-R downstream of C/EBPα.[46]

C/EBPα-C^m or C/EBPα-N^m suppressed the transcriptional activity of C/EBPα-WT by different mechanisms

We next analyzed the transcriptional activation of C/EBPα-WT and mutants in 293T cells using a luciferase construct harboring 2 C/EBPα binding sites. As expected, C/EBPα-WT strongly activated this promoter, while neither C/EBPα-C^m, C/EBPα-N^m, nor C/EBPα-p30 showed any transcriptional activation (Figure 2A). We next examined whether these C/EBPα mutants affected the transcriptional activation of C/EBPα-WT. Although C/EBPα-C^m reduced G-CSF-R expression and inhibited G-CSF–induced myeloid differentiation of 32Dcl3 cells even more efficiently than C/EBPα-N^m (Figure 1D-F), C/EBPα-N^m as well as C/EBPα-p30 but not C/EBPα-C^m decreased promoter activity in the luciferase assay in 293T cells (top panel in Figure 2A), which was in accordance with the data shown by Gombart et al.[20] Expression of C/EBPα WT and mutants in the transfected 293T cells was verified by Western blot analysis (bottom panel in Figure 2A). These results indicated that C/EBPα-C^m and C/EBPα-p30 suppressed expression of G-CSF-R by different mechanisms. Interestingly, transcriptional activation of C/EBPα-WT drastically increased in 293T cells when coexpressed with PU.1, although PU.1 itself did not stimulate the same promoter (top panel in Figure 2B). Notably, this synergistic effect was suppressed by C/EBPα-C^m and weakly by C/EBPα-N^m with low expression levels of p30 protein (top panel in Figure 2B). Expression of C/EBPα and PU.1 was also confirmed by Western blot analysis (bottom panel in Figure 2B). Therefore, we assumed that C/EBPα-C^m was interacting with other transcription factors such as PU.1, thereby suppressing the activation of C/EBPα-WT in hematopoietic cells. We also tested whether the C/EBPα mutants inhibit E2F activity. However, neither C/EBPα-C^m nor C/EBPα-N^m repressed E2F1/DP1-mediated transcription (supplemental Figure 3). In this regard, there was no difference between C/EBPα-C^m and C/EBPα-N^m. We then compared the DNA-binding ability of C/EBPα-WT and mutants by electrophoresis mobility shift assay. As shown in Figure 2C, C/EBPα-WT protein bound to the CSF3R (G-CSF-R) probe, and C/EBPα-p30 protein generated by C/EBPα-N^m less efficiently bound to the same probe. Binding was verified by super-shift of the DNA-protein complex by the anti-C/EBPα Ab. Remarkably, C/EBPα-C^m failed to bind the CSF3R probe (Figure 2C). Next, we examined subcellular localization of C/EBPα-WT and mutants. In line with previous reports, C/EBPα-WT and mutants localized in the nucleus of the interphase cells (Figure 2D). However, it was noteworthy that unlike C/EBPα-WT and C/EBPα-p30, C/EBPα-C^m was not localized on chromosome during the mitotic phase (Figure 2D). It is possible that C/EBPα-C^m without a DNA binding ability is stealing some interacting protein from chromosome. Taken together, these results indicated that C/EBPα-N^m suppressed the transcriptional activation of C/EBPα-WT by its direct binding to the promoter or by its heterodimerization with C/EBPα-WT, while C/EBPα-C^m showed the suppressive effect indirectly, probably through interaction with other transcription factors such as PU.1.

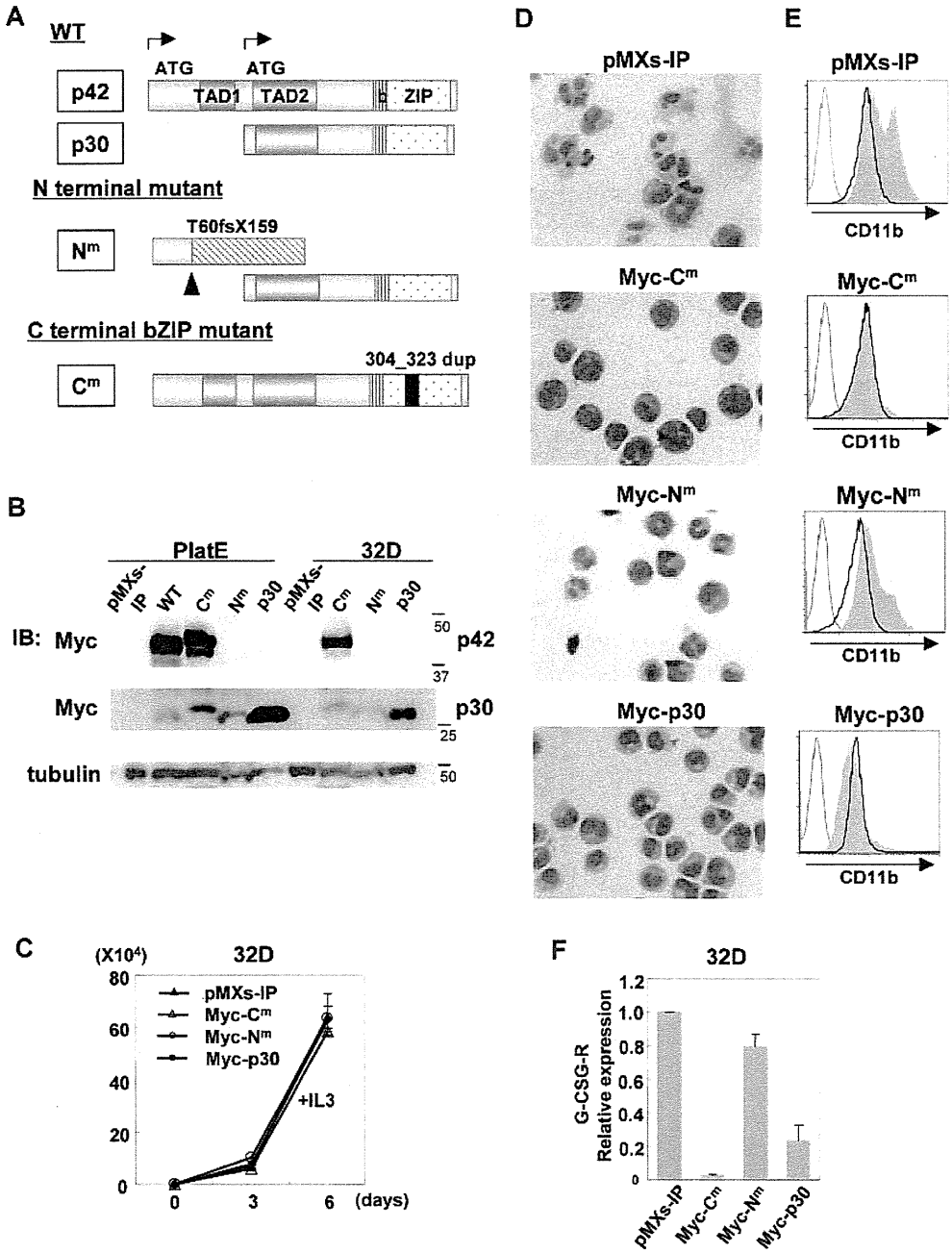

Figure 1. C/EBPα-C^m had the strong ability to block myeloid differentiation. (A) Schematic diagram of C/EBPα-WT (p42 and p30) and mutants, T60fsX159 (C/EBPα-N^m) and 304_323 dup (C/EBPα-C^m). TAD indicates the transcriptional activation domain; bZIP, basic region leucine zipper domain. (B) Expression of C/EBPα-WT and its mutants in Plat-E cells transiently transfected with a Myc-tagged C/EBPα-WT, C/EBPα-C^m, C/EBPα-N^m, or C/EBPα-p30 or an empty vector (pMXs-IP) and expression of C/EBPα mutants in 32Dcl3 cells transduced with Myc-tagged C/EBPα-C^m, C/EBPα-N^m, C/EBPα-p30, or mock (pMXs-IP). Cell lysates were subject to immunoblotting with anti-Myc Ab or anti-tubulin Ab as control. The results shown are representative of 3 independent experiments. (C) The growth of 32Dcl3 cells transduced with Myc-tagged C/EBPα-C^m, C/EBPα-N^m, C/EBPα-p30, or mock (pMXs-IP) in the presence of 1 ng/mL IL-3. All data points correspond to the mean and the standard deviation (SD) of 3 independent experiments. (D-E) 32Dcl3 cells transduced with Myc-tagged C/EBPα-C^m, C/EBPα-N^m, C/EBPα-p30, or mock (pMXs-IP) were cultured in the presence of 50 ng/mL G-CSF for 6 days. (D) Morphology of these cells was assessed by Giemsa staining. Images were obtained with a BX51 microscope and a DP12 camera (Olympus); objective lens, UplanFl (Olympus); original magnification ×40. (E) Surface expression of CD11b in these transfectants after incubation with 1 ng/mL IL-3 (bold histograms) or 50 ng/mL G-CSF (filled histograms) for 6 days was analyzed by flow cytometry. The result of control staining is shown as a thin-lined histogram. Data are representative of 3 independent experiments. (F) Relative expression levels of G-CSF-R in 32Dcl3 cells transduced with Myc-tagged C/EBPα-C^m, C/EBPα-N^m, C/EBPα-p30, or mock (pMXs-IP) were estimated by using real-time PCR. Data are representative of 3 independent experiments.

Retroviral transduction of C/EBPα-C^m, but not C/EBPα-N^m, immortalized BM hematopoietic cells

To determine the effect of C/EBPα-C^m and C/EBPα-N^m on differentiation and proliferation of hematopoietic cells, we performed serial colony-forming assays as described previously.[45] Mouse BM mononuclear cells were transduced with C/EBPα-C^m, C/EBPα-N^m, or C/EBPα-p30. Expression of C/EBPα mutants in the transduced BM cells was verified by Western blot analysis

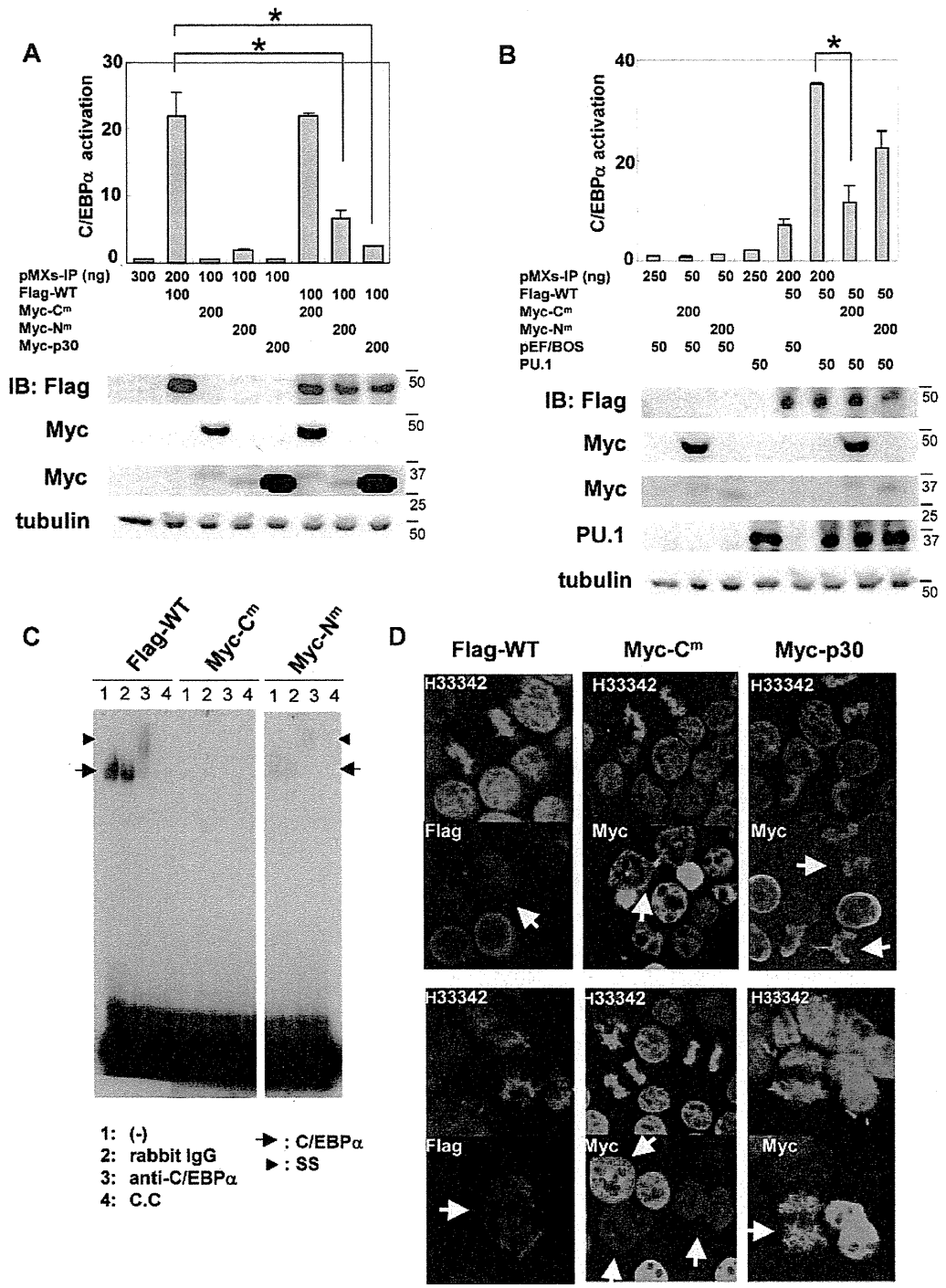

Figure 2. C/EBPα-C^m or C/EBPα-N^m inhibited the transcriptional activation of C/EBPα-WT by different mechanisms. (A-B top) 293T cells were transiently transfected with indicated amounts of expression plasmids (pMXs-Flag-tagged C/EBPα WT-IP, pMXs-Myc-tagged C/EBPα mutants-IP, pMXs-IP, pEF-BOS/PU.1, pEF-BOS) together with 100 ng of the luciferase reporter plasmid p(C/EBP)2TK. The total amount of plasmid for each transfection was adjusted by adding empty plasmids (pMXs-IP or pEF-BOS). Results represented the average values for relative luciferase activity that were normalized using the activity of EF1 vector as an internal control. All transfection groups were normalized with a Renilla luciferase vector as an internal control. All data points correspond to the mean and the standard deviation (SD). Data are representative of 3 independent experiments. Statistically significant differences are shown. *$P < .05$. (Bottom) Expression of C/EBPα-WT, C/EBPα-mutants, or PU.1 in 293T cells transiently transfected as above described. Cell lysates were subject to immunoblotting with anti-Flag Ab, anti-Myc Ab, anti-PU.1 Ab, or anti-tubulin Ab as control. The results shown are representative of 3 independent experiments. (C) DNA binding of C/EBPα-WT and mutants. Electrophoresis mobility shift assay was performed with ^{32}P-labeled oligonucleotides containing the C/EBPα binding site derived from CSF3R promoter and nuclear extracts from 293T cells transiently transfected with pMXs-Flag–tagged C/EBPα WT-IP, pMXs-Myc–tagged C/EBPα-C^m-IP, or pMXs-Myc–tagged C/EBPα-N^m-IP. Data are representative of 3 independent experiments. Lane 1: none (−); lane 2: control rabbit immunoglobulin G was added; lane 3: anti-C/EBPα Ab was added; lane 4: cold competitor (C.C) was added. Ss indicates supershifted bands. (D) 293T cells transiently transfected with pMXs-Flag–tagged C/EBPα-WT-IP, pMXs-Myc-tagged C/EBPα-C^m-IP, or pMXs-Myc–tagged C/EBPα-p30-IP were immunostained with anti-Flag Ab (red) or anti–c-Myc Ab (green) and stained with Hoechst (H33342; blue). Data are representative of 4 independent experiments (total of 15 mitotic cells were examined for each transfectant). Fluorescence images by confocal microscopy were obtained with IX70 (Olympus). Original magnification ×60.

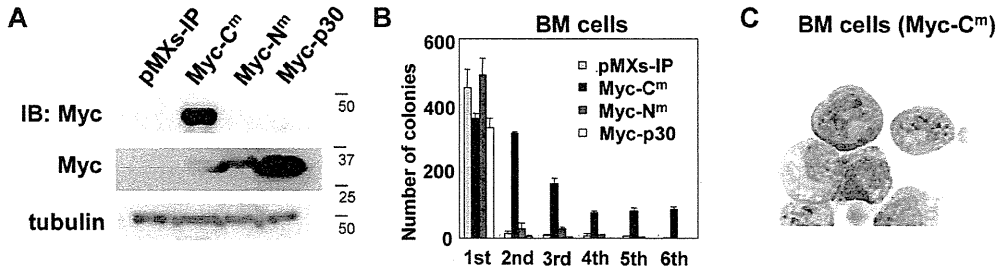

Figure 3. C/EBPα-C^m, but not C/EBPα-N^m, immortalized BM cells. (A) Expression of C/EBPα-C^m, C/EBPα-N^m, or C/EBPα-p30 in BM cells transduced with Myc-tagged C/EBPα-C^m, C/EBPα-N^m, C/EBPα-p30, or mock (pMXs-IP). Cell lysates were subject to immunoblotting with anti-Myc Ab or anti-tubulin Ab as control. The results shown are representative of 3 independent experiments. (B) Colony-forming assay from BM cells transduced with C/EBPα-C^m, C/EBPα-N^m, C/EBPα-p30, or mock (pMXs-IP). Bars represent the number of colonies obtained per 10^4 cells after each round of plating in methylcellulose supplemented with stem cell factor, thrombopoietin, IL-3, and IL-6. Data are representative of 3 independent experiments. All data points correspond to the mean and the standard deviation (SD) of 3 independent experiments. (C) Cytospin preparations of immortalized BM cells transduced with C/EBPα-C^m were stained with Giemsa. Images were obtained with a BX51 microscope and a DP12 camera (Olympus); objective lens, UplanFl (Olympus); original magnification ×100.

(Figure 3A). We also confirmed that the expression levels of p30 protein generated by C/EBPα-p30 are higher than those by C/EBPα-N^m (Figure 3A). Irrespective of different expression levels of p30, most C/EBPα-N^m- and C/EBPα-p30–transduced BM cells did not make secondary colonies after replating (Figure 3B). On the other hand, BM cells expressing C/EBPα-C^m formed colonies after 6 rounds of replating in the presence of cytokine cocktail (Figure 3B). Cytospin preparations of these cells showed blastlike morphologies (Figure 3C). In addition, C/EBPα-C^m–transduced BM cells remained immature and were immortalized in a liquid culture containing IL-3 after several rounds of the replating in semisolid cultures.

Transduction with C/EBPα-C^m into BM cells caused AML in a mouse BMT model

To test whether a single C/EBPα mutant induces hematopoietic abnormality, Ly-5.1 murine BM mononuclear cells, infected with retroviruses harboring C/EBPα-C^m, C/EBPα-N^m, or mock (pMYs-IG), were transplanted into irradiated syngenic Ly-5.2 mice. We confirmed efficient retrovirus infection: 50%-65% of BM cells transduced with C/EBPα-N^m or mock (pMYs-IG) and 35%-50% of BM cells transduced with C/EBPα-C^m were positive for GFP expression before transplantation. Mice receiving transplants of mock (pMYs-IG)–transduced cells (hereafter referred to as mice/pMYs-IG) remained healthy over the observation period (n = 8/8) (Figure 4A). Notably, most of the mice that received transplants of C/EBPα-C^m–transduced cells (hereafter referred to as mice/C^m) developed AML within 4-12 months after transplantation (n = 16/17) (Figure 4A). These morbid mice presented similar phenotypes, characterized by hepatosplenomegaly and pancytopenia (Table 2). BM and spleen were occupied with myeloblasts and myelocytes (Figure 4B). In some cases, leukemic cells displayed morphologic aberrations such as abnormal lobular and ring-shaped nucleus. GFP-positive leukemic cells expressed CD11b and Gr-1 at high levels and c-kit at intermediate to high levels (middle panel in Figure 4C). One of the mice/C^m developed T-cell lymphoma with thymoma (data not shown). We next asked if the integration of retroviruses influenced the outcomes in the BMT model. Southern blot analysis of BM cells of mice/C^m showed a single or several integrations (supplemental Figure 4), and either 1 or 2 integration sites were identified in these samples, based on the inverse PCR method (supplemental Table 1).[47] We found several common integration sites and integrations of the retroviruses in the intron of MN1 in 2 of 15 cases examined (supplemental Table 1). Considering the recent works published by Hasemann et al[48] and by ourselves,[40] retrovirus integration might in part influence the phenotypes of the recipient mice in our BMT models. For example, integration of the retrovirus vector into MN1 may enhance cell growth.[40] However, integration sites do not seem to play major roles in the experiments of this study; C/EBPα-C^m transduction induced AML with similar phenotypes in most cases after a relatively long latency in the BMT model. On the other hand, 5 of 8 mice that received transplants of C/EBPα-N^m–transduced cells (hereafter referred to as mice/N^m) remained healthy during the observation period. Three of 8 mice/N^m developed B-cell acute lymphoblastic leukemia (B-ALL) with hepatosplenomegaly with latencies of 7 to 12 months after transplantation (Figure 4A). BM was occupied with blastlike cells, and the morbid mice exhibited leukocytosis, anemia, and thrombocytopenia (Figure 4B and data not shown). GFP-positive leukemic cells expressed B220 and CD19 at high levels and c-kit at intermediate to high levels (right panel in Figure 4C). One of the mice/N^m developed AML with splenomegaly 13 months after transplantation (data not shown). The reason why C/EBPα-N^m tend to induce B-ALL is not clear. However, we must notice a point that mouse BMT models may not always mimic human diseases.[35,40] Expression of C/EBPα-C^m in spleen cells of mice/C^m with AML or p30 protein generated by C/EBPα-N^m in spleen cells of mice/N^m with B-ALL was confirmed by Western blot analysis (Figure 4D). Collectively, C/EBPα-C^m has a potential to strongly induce AML in a BMT model. Because the latency is relatively long and the leukemic cells seem to be clonal, additional events should have worked with C/EBPα-C^m in inducing leukemia. In addition, the in vivo suppressive effect of C/EBPα-C^m on the activation of endogenous C/EBPα was confirmed by the finding that G-CSF-R expression was down-regulated and c-Myc expression was up-regulated in BM samples of mice/C^m compared with mice/pMYs-IG (Figure 4E-F).

Transduction with both C/EBPα-C^m and C/EBPα-N^m induced more aggressive AML with leucocytosis

To next ask whether the combination of both C/EBPα-C^m and C/EBPα-N^m would induce AML more efficiently, we performed BMT, using murine BM mononuclear cells infected with retroviruses harboring Myc-tagged C/EBPα-C^m-IRES-GFP and Flag-tagged C/EBPα-N^m-IRES-dsRED. BM mononuclear cells expressing both mutants were recognized as GFP- and dsRED-double positive cells, 10%-22% of BM cells before the transplantation. Notably, mice that had received transplants of BM cells expressing both mutants (hereafter referred to as mice/Myc-C^m/Flag-N^m) developed AML with hepatosplenomegaly with shorter latencies

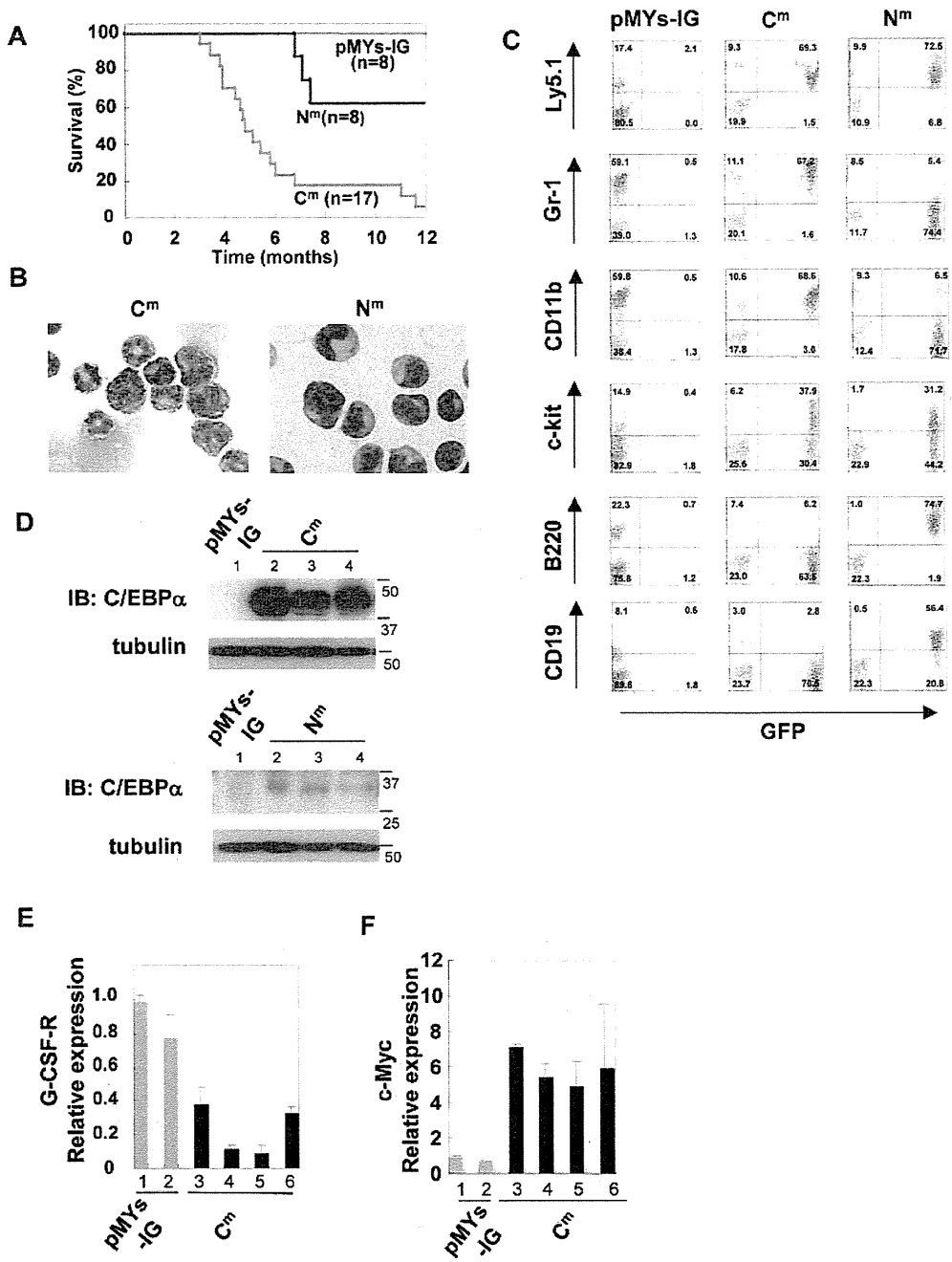

Figure 4. Transduction with C/EBPα-C^m alone induced AML in a mouse BMT model. (A) Kaplan-Meier analysis for the survival of mice that received transplants of BM cells transduced with C/EBPα-C^m-IG (C^m, n = 17), C/EBPα-N^m-IG (N^m, n = 8), or mock (pMYs-IG, n = 8). (B) Cytospin preparations of BM cells derived from mice/C/EBPα-C^m (left) or mice/N^m (right) were stained with Giemsa. A representative photograph is shown. Images were obtained with a BX51 microscope and a DP12 camera (Olympus); objective lens, UplanFl (Olympus); original magnification ×100. (C) Flow cytometric analysis of BM cells derived from mice/C/EBPα-C^m (middle), mice/C/EBPα-N^m (right), or mice/pMYs-IG (left). The dot plots show Ly5.1, Gr-1, CD11b, c-kit, B220, or CD19 labeled with phycoerythrin-conjugated monoclonal Ab versus expression of GFP. (D) Expression of C/EBPα-C^m protein and p30 protein generated by C/EBPα-N^m in spleen cells of mice/pMYs-IG (lane 1) and mice/C^m (lanes 2-4) (top) or in spleen cells of mice/pMYs-IG (lane 1) and mice/N^m (lanes 2-4) (bottom). Cell lysates were subject to immunoblotting with anti-C/EBPα (14AA) Ab or anti-tubulin Ab as control. Data are representative of 3 independent experiments. (E-F) Real-time PCR for G-CSF-R (E) or c-Myc (F) in BM cells derived from mice/C^m or mice/pMYs-IG. Expression levels were normalized by β-actin mRNA. The relative expression level of BM derived from mice/mock (lane 1) was defined as 1. All data points correspond to the mean and the standard deviation (SD) of 3 independent experiments. Lanes 1-2: mice/pMYs-IG; lanes 3-6: mice/C^m.

(3-5 months) compared with mice that had received transplants of BM cells expressing both Myc-C^m-IRES-GFP and mock (pMYs-IR, hereafter referred to as mice/Myc-C^m/pMYs-IR; Figure 5A). Of note, there was no significant difference of the phenotypes between mice/C^m and mice/Myc-C^m/pMYs-IR or between mice/N^m and mice that had received transplants of BM cells expressing both mock (pMYs-IG) and Flag-N^m-IRES-dsRED (hereafter referred to as mice/pMYs-IG/Flag-N^m; Figures 4-5 and data not shown). The percentages of the immature blast ranged from 72%-94% in mice/Myc-C^m/Flag-N^m (Table 2) compared with 62%-92% in

Table 2. Characteristics of AML caused by C/EBPα mutants

	pMYs-IG/pMYs-IR (n = 8)	Myc-C^m/pMYs-IR (n = 6)	Myc-C^m/Flag-N^m (n = 8)
WBC (/μL)	9060 ± 1648	5816 ± 3128	36 675 ± 22 956
Hb (g/dL)	16.4 ± 3.2	12.4 ± 2.2	10.7 ± 2.3
Plt (× 10^4/μL)	79.4 ± 43.1	7.2 ± 4.5	19.8 ± 13.1
BM count (× 10^7)	3.34 ± 0.73	1.69 ± 0.30	2.83 ± 0.88
Leukemic cells (%)	-	60-92	72-94
Liver weight (mg)	1433 ± 153	2071 ± 1281	2441 ± 1315
Spleen weight (mg)	113 ± 24	476 ± 220	549 ± 239

Averages and standard deviations are shown. BM cells were isolated from both tibias and femurs.

WBC indicates white blood cell; Hb, hemoglobin; and Plt, platelets.

C/EBPα-C^m–induced leukemia (Table 2 and Figure 5B). Morphologies of the leukemic blasts are more immature in mice/Myc-C^m/Flag-N^m than mice/Myc-C^m/pMYs-IR (Figure 5B), consistent with the lower expression of Gr-1 in the former (Figure 5C and data not shown). Flow cytometric analysis delineated that most leukemic cells of mice/Myc-C^m/Flag-N^m expressed both GFP and dsRED (Figure 5C) and invariable markers: CD11b-inntermediate and Gr-1, B-220, c-kit-low (Figure 5C). Expression of both C/EBPα-C^m protein and p30 protein generated by C/EBPα-N^m in leukemic cells of mice/Myc-C^m/Flag-N^m was confirmed by Western blot analysis (Figure 5D). Expression levels of p30 protein generated by C/EBPα-N^m were not correlated with the disease latency in mice/Myc-C^m/Flag-N^m (Figure 5A,D). The morbid mice/Myc-C^m/Flag-N^m suffered from anemia and thrombocytopenia-like mice/Myc-C^m/pMYs-IR; however, it was of note that unlike mice/Myc-C^m/pMYs-IR, most mice/Myc-C^m/Flag-N^m exhibited marked leukocytosis (Figure 5E-F and Table 2). These results suggested that C/EBPα-N^m either confers a proliferative advantage on immature myeloid cells or collaborates with C/EBPα-C^m in blocking differentiation of myeloid cells in vivo. It is of note that this collaborative effect was induced by relatively low levels of p30 protein generated by C/EBPα-N^m.

C/EBPα-C^m, but not C/EBPα-N^m, collaborated with Flt3-ITD in inducing AML in a BMT model

Because C/EBPα-C^m possessed the potential to strongly suppress myeloid differentiation, this mutation could be categorized into class II mutations. We speculated that AML would be efficiently induced by combining C/EBPα-C^m with class I gene alterations. To test this, murine BM mononuclear cells, transduced with both Flt3-ITD and either C/EBPα-C^m or C/EBPα-N^m, were transplanted into the recipient mice. BM mononuclear cells expressing both mutants were recognized as GFP- and dsRED-double positive cells, 10%-20% of BM cells before the transplantation. As reported previously,[49] mice receiving transplants of BM cells expressing both Flt3-ITD-IRES-GFP and mock (pMYs-IR) (mice/FLT/pMYs-IR) developed myeloproliferative neoplasm (MPN) within 1.5-3 months after transplantation (Figure 6A). BM and spleen were occupied with increased numbers of mature myeloid cells expressing CD11b at high levels and Gr-1 at intermediate to high levels (Figure 6B-C). Intriguingly, mice transplanted with BM cells expressing both Flt3-ITD-IRES-GFP and C/EBPα-C^m-IRES-dsRED (mice/FLT/C^m) developed aggressive leukemia within 2-3 weeks after transplantation (Figure 6A). Histologic examination of mice/FLT/C^m showed that BM was occupied with the 2 populations: large and small blastlike cells (Figure 6B). However, flow cytometric analysis demonstrated that both populations, double positive for GFP and dsRED, similarly expressed B220, CD19, Gr-1, and CD11b and could not be differentiated (Figure 6C and data not shown). Thus, mice/FLT/C^m invariably developed biphenotypic leukemia. Western blot analysis demonstrated that both Flt3-ITD and C/EBPα-C^m proteins were expressed in spleen cells of mice/FLT/C^m (Figure 6D). On the other hand, mice that received transplants of BM cells expressing both Flt3-ITD-IRES-GFP and C/EBPα-N^m-IRES-dsRED (mice/FLT/N^m) developed MPN with latencies comparable with those of MPN developed by mice/FLT/pMYs-IR, although some lymphoid blast cells were observed in 2 mice/FLT/N^m (Figure 6A and data not shown). Thus, C/EBPα-N^m did not significantly collaborate with Flt3-ITD in leukemogenesis in the present BMT model. Finally, leukemic cells derived from mice/FLT/C^m proliferated independently of IL-3 in the culture, while those from mice/C^m still required IL-3 for their growth. Leukemic cells derived from mice/FLT or mice/FLT/N^m did not survive even in the presence of IL-3. Moreover, we found stronger activation of STAT5, STAT3, AKT, and ERK in leukemic cell lines derived from mice/C^m/FLT compared with those from mice/C^m (Figure 6E). These results indicated that Flt3-ITD conferred additional proliferative potentials as a class I mutation on the cells expressing C/EBPα-C^m alone, thereby inducing aggressive leukemia.

Discussion

The present results on *CEBPA* mutations of AML patients confirmed previous reports[20-28]; *CEBPA* mutations are found in 5%-14% of de novo AML, and most of them harbor 2 distinct mutations on different alleles and have good prognosis. In addition, our results suggested that mutations of *CEBPA* are found only in one allele in most cases of therapy-related AML or MDS, and AML progressed from MDS harboring CEBPA mutations (8/71 and 7/224). While we did not find additional mutations in other genes in de novo AML patients with double CEBPA mutations, we detected 3 additional mutations in 15 patients with therapy-related AML or MDS and MDS/AML. These results indicate that a *CEBPA* mutation collaborates with either a different type of CEBPA mutations or mutations in different genes in inducing leukemia.

Analysis of CEBPA mutations in in vitro assays provided novel insights concerning the role of CEBPα in blood cells. C/EBPα-N^m and p30, but not C/EBPα-C^m, suppressed transcriptional activation of C/EBPα-WT in a luciferase assay using 293T cells (Figure 2A) as reported previously.[20] Curiously, expression of G-CSF-R, a major target of C/EBPα, was profoundly suppressed by C/EBPα-C^m but not by C/EBPα-N^m in 32Dcl3 cells (Figure 1F). C/EBPα-C^m suppressed G-CSF–induced granulocytic differentiation of 32Dcl3 cells more efficiently than C/EBPα-N^m (Figure 1D-E). It is possible that insufficient suppression of G-CSF–induced differentiation of 32Dcl3 cells by C/EBPα-N^m despite its inhibitory activity on transcriptional activation of C/EBPα-WT in 293T cells may be because of the low expression of C/EBPα-N^m in 32Dcl3 cells (Figure 1B). In fact, C/EBPα-p30 moderately suppressed the expression of G-CSF-R and inhibited G-CSF–induced differentiation of 32Dcl3 cells (Figure 1D-F). However, this does not explain why C/EBPα-C^m efficiently blocks the differentiation of 32Dcl3 cells despite its inability to suppress C/EBPα activation in the luciferase assay. Therefore, we speculated that C/EBPα mutants behave differently in epithelial 293T cells and hematopoietic 32Dcl3 cells and tested whether hemotopoietic cell–specific transcription factors play some role in 32Dcl3 cells. Because it was